Appl. Math. Mech. -Engl. Ed., **40**(12), 1695–1722 (2019)

Applied Mathematics and Mechanics (English Edition)

https://doi.org/10.1007/s10483-019-2549-7

A nonlocal strain gradient shell model incorporating surface effects for vibration analysis of functionally graded cylindrical nanoshells*

Lu LU[1,2], Li ZHU[3], Xingming GUO[1,†], Jianzhong ZHAO[1], Guanzhong LIU[1]

1. Shanghai Institute of Applied Mathematics and Mechanics, Shanghai Key Laboratory of Mechanics in Energy Engineering, School of Mechanics and Engineering Science, Shanghai University, Shanghai 200072, China;
2. Department of Mechanical Engineering, University of Alberta, Edmonton T6G 2G8, Canada;
3. School of Mathematics and Computational Sciences, Xiangtan University, Xiangtan 411105, Hunan Province, China

(Received Jul. 3, 2019 / Revised Aug. 10, 2019)

Abstract In this paper, a novel size-dependent functionally graded (FG) cylindrical shell model is developed based on the nonlocal strain gradient theory in conjunction with the Gurtin-Murdoch surface elasticity theory. The new model containing a nonlocal parameter, a material length scale parameter, and several surface elastic constants can capture three typical types of size effects simultaneously, which are the nonlocal stress effect, the strain gradient effect, and the surface energy effects. With the help of Hamilton's principle and first-order shear deformation theory, the non-classical governing equations and related boundary conditions are derived. By using the proposed model, the free vibration problem of FG cylindrical nanoshells with material properties varying continuously through the thickness according to a power-law distribution is analytically solved, and the closed-form solutions for natural frequencies under various boundary conditions are obtained. After verifying the reliability of the proposed model and analytical method by comparing the degenerated results with those available in the literature, the influences of nonlocal parameter, material length scale parameter, power-law index, radius-to-thickness ratio, length-to-radius ratio, and surface effects on the vibration characteristic of functionally graded cylindrical nanoshells are examined in detail.

Key words nonlocal strain gradient theory, surface elasticity theory, first-order shear deformation theory, vibration, functionally graded (FG) cylindrical nanoshell

Chinese Library Classification O344
2010 Mathematics Subject Classification 74A20, 74H45, 74K25

* Citation: LU, L., ZHU, L., GUO, X. M., ZHAO, J. Z., and LIU, G. Z. A nonlocal strain gradient shell model incorporating surface effects for vibration analysis of functionally graded cylindrical nanoshells. *Applied Mathematics and Mechanics* (*English Edition*), **40**(12), 1695–1722 (2019) https://doi.org/10.1007/s10483-019-2549-7

† Corresponding author, E-mail: xmguo@shu.edu.cn

Project supported by the National Natural Science Foundation of China (Nos. 11872233 and 11472163), the China Scholarship Council (No. 201706890041), and the Innovation Program of Shanghai Municipal Education Commission (No. 2017-01-07-00-09-E00019)

1 Introduction

Functionally graded (FG) materials are an advanced class of composite structures with material properties changing continuously in one or more directions. In recent years, with the rapid development of nanotechnology, FG nanoscale and microscale structures with potential applications in nanoelectromechanical systems (NEMS) and microelectromechanical systems (MEMS) have attracted a great deal of attention. Consequently, investigating the size-dependent mechanical behaviors of FG nano-/micro-structures is of great importance for better understanding and designing those small-scaled systems. Since the experimental study in nanoscale may be technically difficult and financially expensive, and molecular dynamics simulation is time-consuming for analyzing large size system, the continuum mechanics approach, as an alternative way to model the mechanical response of nano-/micro-structures, has been widely used. It is well-known that classical continuum mechanics is size-independent and cannot capture the size effects in small scale. In this regard, several non-classical continuum theories have been developed to assess the remarkable size effects on the mechanical characteristics of nano-/micro-structures, such as nonlocal elasticity theory[1–2], strain gradient elasticity theory[3–6], and surface elasticity theory[7–8].

Based on the nonlocal elasticity theory and strain gradient elasticity theory, a large number of works on the size-dependent analysis of nano-/micro-structures have been carried out in the last two decades (see review articles [9]–[11]), these works have shown that the nonlocal theory captures only the stiffness-softening effect and the strain gradient theory captures only the stiffness-hardening effect. Recently, the nonlocal elasticity theory and strain gradient elasticity theory have been combined into a single theory, namely, the nonlocal strain gradient theory (NSGT)[12]. NSGT takes not only the nonlocal stress field but also the strain gradient stress field into account, which is capable of describing both stiffness-softening effect and stiffness-hardening effect. Based upon the NSGT, numerous works have been performed to investigate the size-dependent linear or nonlinear bending, buckling, vibration, and wave propagation of FG small-scaled beams[13–24], plates[25–32], and shells[33–37]. To mention a few, She et al.[38] analyzed the wave propagation of porous FG nanotubes with the help of NSGT and a refined beam model. Sobhy and Zenkour[39] investigated the buckling and vibration behaviors of a double-layered FG porous nanoplate via NSGT in conjunction with a quasi-3D refined theory. Moreover, by using NSGT and first-order shear deformation shell theory, the free and forced vibrations of porous FG cylindrical nanoshells were studied by Barati[40] and Faleh et al.[41], respectively. In another work, Ma et al.[42] investigated the wave propagation characteristics in magneto-electro-elastic nanoshells within the framework of NSGT.

On the other hand, it is known that for a solid with large surface area to bulk volume ratio, the atom arrangement and material properties of the surface are different from those in the bulk part, which makes the mechanical behavior of the solid become unusual compared with conventional structures. To capture the surface effects, Gurtin and Murdoch[7–8] proposed the surface elasticity theory, which defines the surface as a membrane without thickness, and suggests that the surface has different material properties and constitutive relations than the bulk part. Based on the surface elasticity theory, a large amount of research has focused on the analysis of surface effects on the mechanical response of FG nanostructures[43–52]. For example, Zhu et al.[53] investigated surface energy effects on the torsional buckling of FG cylindrical nanoshells covered with piezoelectric nano-layers based on the surface elasticity theory. Norouzzadeh and Ansari[54] analyzed the size-dependent vibration characteristics of FG rectangular and circular nanoplates in the framework of nonlocal elasticity and surface elasticity theories. In a recent work, Attia and Abdel-Rahman[55] studied the simultaneous effects of the microstructure rotation and surface energy on the vibration of FG viscoelastic nanobeams by using the modified couple stress theory and surface elasticity theory.

From the above-mentioned, we can find that NSGT and surface elasticity theory describe

the remarkable size effects at small scale in totally different ways. Therefore, there is a scientific need to explore the combined effects of nonlocal stress, strain gradient, and surface energy by using NSGT in conjunction with the surface elasticity theory. Recently, the combined effect of nonlocal stress, strain gradient, and surface energy on the mechanical behaviors of homogenous nanoplates and nanoshells have been addressed by some researchers[56–58]. However, to the best of the authors' knowledge, no works have been concerned with combining NSGT with surface elasticity theory to assess the size effects in FG nanoshells so far.

In this regard, the primary objective of the present work is to develop a nonlocal strain gradient shell model including surface effects for the size-dependent analysis of FG cylindrical nanoshells. To achieve this goal, firstly, NSGT in conjunction with surface elasticity theory will be applied to establish the governing equations in Section 2. Afterwards, closed-form solutions for the free vibration problem will be formulated in Section 3. Then, a comparative study is performed in Section 4 to examine the validity of the proposed model and the accuracy of the analytical method. Next, the effects of various parameters, such as nonlocal parameter, material length scale parameter, radius-to-thickness ratio, length-to-radius ratio, power-law index, and surface energy on the vibration response of FG cylindrical nanoshells are investigated in Section 5. Finally, the main conclusions of the present work are summarized in Section 6.

2 Nonlocal strain gradient shell model incorporating surface effects

As depicted in Fig. 1, an FG cylindrical nanoshell of length L, thickness h, and radius R is considered. The coordinate system (x, θ, z) is established in the mid-plane of the nanoshell, and the x-, θ-, and z-axes are taken along the axial, circumferential, and radical directions, respectively. It is assumed that the FG cylindrical nanoshell is made of a mixture of ceramics and metals, and the material properties vary continuously from metals at the inner surface ($z=-h/2$) to ceramics at the outer surface ($z=h/2$) along the thickness direction according to a power-law distribution. Thus, the effective Young's modulus $E(z)$, effective Poisson's ratio $\mu(z)$, and effective mass density $\rho(z)$ of the FG cylindrical nanoshell can be written as follows[59]:

$$\begin{cases} E(z) = (E_{\rm c} - E_{\rm m})\Big(\dfrac{z}{h} + \dfrac{1}{2}\Big)^{\xi} + E_{\rm m}, \\ \mu(z) = (\mu_{\rm c} - \mu_{\rm m})\Big(\dfrac{z}{h} + \dfrac{1}{2}\Big)^{\xi} + \mu_{\rm m}, \\ \rho(z) = (\rho_{\rm c} - \rho_{\rm m})\Big(\dfrac{z}{h} + \dfrac{1}{2}\Big)^{\xi} + \rho_{\rm m}, \end{cases} \tag{1}$$

where ξ is the power-law index ($0 \leqslant \xi < \infty$). The subscripts "c" and "m" stand for the ceramic and metal constituents, respectively.

2.1 Kinematics

Based on the FSDT, the displacement field of a cylindrical shell is given by

$$\begin{cases} u_x(x,\theta,z,t) = u(x,\theta,t) + z\varphi_x(x,\theta,t), \\ u_\theta(x,\theta,z,t) = v(x,\theta,t) + z\varphi_\theta(x,\theta,t), \\ u_z(x,\theta,z,t) = w(x,\theta,t), \end{cases} \tag{2}$$

where $u(x,\theta,t)$, $v(x,\theta,t)$, and $w(x,\theta,t)$ are the displacements in axial, circumferential, and radical directions, respectively. $\varphi_x(x,\theta,t)$ and $\varphi_\theta(x,\theta,t)$ represent the rotations about θ- and x-axes, respectively. Accordingly, the strain field can be written as

$$\varepsilon_{xx} = \frac{\partial u}{\partial x} + z\frac{\partial \varphi_x}{\partial x}, \quad \varepsilon_{\theta\theta} = \frac{1}{R}\frac{\partial v}{\partial \theta} + \frac{z}{R}\frac{\partial \varphi_\theta}{\partial \theta} + \frac{w}{R}, \tag{3}$$

$$\gamma_{x\theta} = \frac{1}{R}\frac{\partial u}{\partial \theta} + \frac{\partial v}{\partial x} + \frac{z}{R}\frac{\partial \varphi_x}{\partial \theta} + z\frac{\partial \varphi_\theta}{\partial x}, \quad \gamma_{xz} = \varphi_x + \frac{\partial w}{\partial x}, \quad \gamma_{\theta z} = \varphi_\theta + \frac{1}{R}\frac{\partial w}{\partial \theta} - \frac{v}{R}. \tag{4}$$

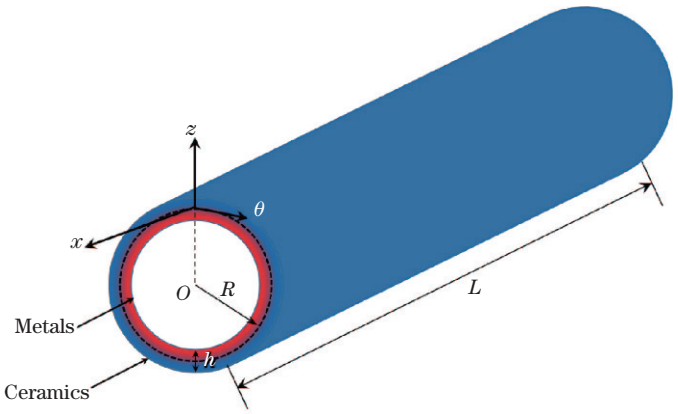

Fig. 1 Schematic diagram of an FG cylindrical nanoshell (color online)

2.2 Constitutive relations

In the current work, constitutive relations of the FG cylindrical nanoshell including surface effects are established within the framework of NSGT. To account for surface effects, the surface elasticity theory proposed by Gurtin and Murdoch[7–8] is applied. According to the surface elasticity theory, the FG cylindrical nanoshell is assumed to be composed of a bulk part and two thin surface layers (inner surface $z=-h/2$ and outer surface $z=h/2$). The two surface layers are treated as zero thickness films, and perfectly adhere to the underlying bulk material without slipping. In doing this, the constitutive relations of the two surface layers are introduced as

$$\begin{cases} \sigma_{\alpha\beta}^{\mathrm{s}\pm}=\tau^{\mathrm{s}\pm}\delta_{\alpha\beta}+(\tau^{\mathrm{s}\pm}+\lambda^{\mathrm{s}\pm})\varepsilon_{\gamma\gamma}^{\pm}\delta_{\alpha\beta}+2(\mu^{\mathrm{s}\pm}-\tau^{\mathrm{s}\pm})\varepsilon_{\alpha\beta}^{\pm}+\tau^{\mathrm{s}\pm}u_{\alpha,\beta}^{\mathrm{s}\pm}, \\ \sigma_{\alpha z}^{\mathrm{s}\pm}=\tau^{\mathrm{s}\pm}u_{z,\alpha}^{\mathrm{s}\pm}, \quad \alpha,\beta=x,\theta, \end{cases} \tag{5}$$

where $\lambda^{\mathrm{s}\pm}$ and $\mu^{\mathrm{s}\pm}$ denote the surface Lamé constants, $\tau^{\mathrm{s}\pm}$ represents the surface residual stress, and $\delta_{\alpha\beta}$ is the Kronecker delta. Note that the superscript s$\pm$ stand for the outer surface and inner surface, respectively.

In surface elasticity theory, the surface balance conditions cannot be satisfied due to the fact that the stress component σ_{zz} is usually neglected in classical continuum mechanics. To improve this weakness, following Lu et al.[60], it is assumed that σ_{zz} varies linearly through the thickness and satisfies the surface balance conditions, and therefore σ_{zz} is expressed as

$$\begin{aligned} \sigma_{zz}=&\frac{1}{2}\Big(\Big(\frac{\partial\sigma_{xz}^{\mathrm{s}+}}{\partial x}+\frac{1}{R}\frac{\partial\sigma_{\theta z}^{\mathrm{s}+}}{\partial\theta}-\rho^{\mathrm{s}+}\frac{\partial^2 w}{\partial t^2}\Big)+\Big(\rho^{\mathrm{s}-}\frac{\partial^2 w}{\partial t^2}-\frac{\partial\sigma_{xz}^{\mathrm{s}-}}{\partial x}-\frac{1}{R}\frac{\partial\sigma_{\theta z}^{\mathrm{s}-}}{\partial\theta}\Big)\Big) \\ &+\frac{z}{h}\Big(\Big(\frac{\partial\sigma_{xz}^{\mathrm{s}+}}{\partial x}+\frac{1}{R}\frac{\partial\sigma_{\theta z}^{\mathrm{s}+}}{\partial\theta}-\rho^{\mathrm{s}+}\frac{\partial^2 w}{\partial t^2}\Big)-\Big(\rho^{\mathrm{s}-}\frac{\partial^2 w}{\partial t^2}-\frac{\partial\sigma_{xz}^{\mathrm{s}-}}{\partial x}-\frac{1}{R}\frac{\partial\sigma_{\theta z}^{\mathrm{s}-}}{\partial\theta}\Big)\Big). \end{aligned} \tag{6}$$

By substituting Eq. (5) into Eq. (6), σ_{zz} can be rewritten as

$$\begin{aligned} \sigma_{zz}=&\Big(\frac{1}{2}(\tau^{\mathrm{s}+}-\tau^{\mathrm{s}-})+\frac{z}{h}(\tau^{\mathrm{s}+}+\tau^{\mathrm{s}-})\Big)\Big(\frac{\partial^2 w}{\partial x^2}+\frac{1}{R^2}\frac{\partial^2 w}{\partial\theta^2}\Big) \\ &-\Big(\frac{1}{2}(\rho^{\mathrm{s}+}-\rho^{\mathrm{s}-})+\frac{z}{h}(\rho^{\mathrm{s}+}+\rho^{\mathrm{s}-})\Big)\frac{\partial^2 w}{\partial t^2}, \end{aligned} \tag{7}$$

in which $\rho^{\mathrm{s}+}$ and $\rho^{\mathrm{s}-}$ are the surface mass densities of the outer surface and inner surface, respectively.

By taking σ_{zz} into account, the constitutive relations of the bulk part in surface elasticity theory are given by[60]

$$\sigma_{\alpha\beta}=\frac{E(z)}{1+\mu(z)}\Big(\varepsilon_{\alpha\beta}+\frac{\mu(z)}{1-\mu(z)}\varepsilon_{\gamma\gamma}\delta_{\alpha\beta}\Big)+\frac{\mu(z)}{1-\mu(z)}\sigma_{zz}\delta_{\alpha\beta}. \tag{8}$$

On the other hand, the constitutive relation with the framework of NSGT is written as[12]

$$\big(1-(ea)^2\nabla^2\big)\,t_{ij}=(1-l^2\nabla^2)C_{ijkl}\varepsilon_{kl}, \tag{9}$$

where $\nabla^2=\frac{\partial^2}{\partial x^2}+\frac{1}{R^2}\frac{\partial^2}{\partial\theta^2}$ is the Laplacian operator in cylindrical coordinate system, t_{ij} is the total stress, C_{ijkl} is the elastic modulus, and ε_{kl} is the strain. (ea) is the nonlocal parameter introduced to describe the nonlocal effect, and l is the material length scale parameter involved to capture the strain gradient effect. It is seen that the remarkable nonlocal effect and strain gradient effect in small scale can be captured by the NSGT simultaneously.

By applying Eq. (9) to both the bulk part and two surface layers of the FG cylindrical nanoshell, and substituting Eqs. (3) and (4) into the stress components, the constitutive equations based on the NSGT including surface effects can be obtained as follows:

$$\begin{aligned}\big(1-(ea)^2\nabla^2\big)\,t_{xx}=&(1-l^2\nabla^2)\Big(\frac{E(z)}{1-\mu(z)^2}\Big(\frac{\partial u}{\partial x}+z\frac{\partial\varphi_x}{\partial x}+\mu(z)\Big(\frac{1}{R}\frac{\partial v}{\partial\theta}+\frac{z}{R}\frac{\partial\varphi_\theta}{\partial\theta}+\frac{w}{R}\Big)\Big)\\&+\frac{\mu(z)}{1-\mu(z)}\Big(\Big(\frac{1}{2}(\tau^{s+}-\tau^{s-})+\frac{z}{h}(\tau^{s+}+\tau^{s-})\Big)\Big(\frac{\partial^2 w}{\partial x^2}+\frac{1}{R^2}\frac{\partial^2 w}{\partial\theta^2}\Big)\\&-\Big(\frac{1}{2}(\rho^{s+}-\rho^{s-})+\frac{z}{h}(\rho^{s+}+\rho^{s-})\Big)\frac{\partial^2 w}{\partial t^2}\Big)\Big),\end{aligned} \tag{10}$$

$$\begin{aligned}\big(1-(ea)^2\nabla^2\big)\,t_{\theta\theta}=&(1-l^2\nabla^2)\Big(\frac{E(z)}{1-\mu(z)^2}\Big(\mu(z)\Big(\frac{\partial u}{\partial x}+z\frac{\partial\varphi_x}{\partial x}\Big)+\frac{1}{R}\frac{\partial v}{\partial\theta}+\frac{z}{R}\frac{\partial\varphi_\theta}{\partial\theta}+\frac{w}{R}\Big)\\&+\frac{\mu(z)}{1-\mu(z)}\Big(\Big(\frac{1}{2}(\tau^{s+}-\tau^{s-})+\frac{z}{h}(\tau^{s+}+\tau^{s-})\Big)\Big(\frac{\partial^2 w}{\partial x^2}+\frac{1}{R^2}\frac{\partial^2 w}{\partial\theta^2}\Big)\\&-\Big(\frac{1}{2}(\rho^{s+}-\rho^{s-})+\frac{z}{h}(\rho^{s+}+\rho^{s-})\Big)\frac{\partial^2 w}{\partial t^2}\Big)\Big),\end{aligned} \tag{11}$$

$$\big(1-(ea)^2\nabla^2\big)\,t_{x\theta}=\frac{E(z)}{2(1+\mu(z))}(1-l^2\nabla^2)\Big(\frac{1}{R}\frac{\partial u}{\partial\theta}+\frac{\partial v}{\partial x}+\frac{z}{R}\frac{\partial\varphi_x}{\partial\theta}+z\frac{\partial\varphi_\theta}{\partial x}\Big), \tag{12}$$

$$\big(1-(ea)^2\nabla^2\big)\,t_{xz}=\frac{E(z)}{2(1+\mu(z))}(1-l^2\nabla^2)\Big(\varphi_x+\frac{\partial w}{\partial x}\Big), \tag{13}$$

$$\big(1-(ea)^2\nabla^2\big)\,t_{\theta z}=\frac{E(z)}{2(1+\mu(z))}(1-l^2\nabla^2)\Big(\varphi_\theta+\frac{1}{R}\frac{\partial w}{\partial\theta}-\frac{v}{R}\Big), \tag{14}$$

$$\begin{aligned}\big(1-(ea)^2\nabla^2\big)\,t^{s\pm}_{xx}=&(1-l^2\nabla^2)\Big((\lambda^{s\pm}+2\mu^{s\pm})\Big(\frac{\partial u}{\partial x}\pm\frac{h}{2}\frac{\partial\varphi_x}{\partial x}\Big)\\&+(\lambda^{s\pm}+\tau^{s\pm})\Big(\frac{1}{R}\frac{\partial v}{\partial\theta}\pm\frac{h}{2R}\frac{\partial\varphi_\theta}{\partial\theta}+\frac{w}{R}\Big)+\tau^{s\pm}\Big),\end{aligned} \tag{15}$$

$$\begin{aligned}\big(1-(ea)^2\nabla^2\big)\,t^{s\pm}_{\theta\theta}=&(1-l^2\nabla^2)\Big((\lambda^{s\pm}+\tau^{s\pm})\Big(\frac{\partial u}{\partial x}\pm\frac{h}{2}\frac{\partial\varphi_x}{\partial x}\Big)\\&+(\lambda^{s\pm}+2\mu^{s\pm})\Big(\frac{1}{R}\frac{\partial v}{\partial\theta}\pm\frac{h}{2R}\frac{\partial\varphi_\theta}{\partial\theta}+\frac{w}{R}\Big)-\frac{w}{R}\tau^{s\pm}+\tau^{s\pm}\Big),\end{aligned} \tag{16}$$

$$\left(1-(ea)^2\nabla^2\right)t_{x\theta}^{\mathrm{s}\pm}=(1-l^2\nabla^2)\Big(\mu^{\mathrm{s}\pm}\Big(\frac{1}{R}\frac{\partial u}{\partial\theta}\pm\frac{h}{2R}\frac{\partial\varphi_x}{\partial\theta}\Big)+(\mu^{\mathrm{s}\pm}-\tau^{\mathrm{s}\pm})\Big(\frac{\partial v}{\partial x}\pm\frac{h}{2}\frac{\partial\varphi_\theta}{\partial x}\Big)\Big),\quad(17)$$

$$\left(1-(ea)^2\nabla^2\right)t_{\theta x}^{\mathrm{s}\pm}=(1-l^2\nabla^2)\Big(\mu^{\mathrm{s}\pm}\Big(\frac{\partial v}{\partial x}\pm\frac{h}{2}\frac{\partial\varphi_\theta}{\partial x}\Big)+(\mu^{s\pm}-\tau^{s\pm})\Big(\frac{1}{R}\frac{\partial u}{\partial\theta}\pm\frac{h}{2R}\frac{\partial\varphi_x}{\partial\theta}\Big)\Big),\quad(18)$$

$$\left(1-(ea)^2\nabla^2\right)t_{xz}^{\mathrm{s}\pm}=\tau^{\mathrm{s}\pm}(1-l^2\nabla^2)\frac{\partial w}{\partial x},\quad(19)$$

$$\left(1-(ea)^2\nabla^2\right)t_{\theta z}^{\mathrm{s}\pm}=\tau^{\mathrm{s}\pm}(1-l^2\nabla^2)\frac{1}{R}\frac{\partial w}{\partial\theta}.\quad(20)$$

2.3 Variational formulation

The equilibrium equations for the vibration of FG cylindrical nanoshell will be formulated using Hamilton's principle. According to the Hamilton's principle, one can get that

$$\int_0^t(\delta K-\delta U+\delta W)\mathrm{d}t=0,\quad(21)$$

where δU, δK, and δW are the first variation of strain energy, kinetic energy, and work done by external forces, respectively. Due to the surface effects, the strain energy should include both the bulk part and two surface layers. Thus, we have

$$\begin{aligned}\delta U&=\int_V t_{ij}\delta\varepsilon_{ij}\mathrm{d}V+\int_{\mathrm{s}+}t_{ij}^{\mathrm{s}+}\delta\varepsilon_{ij}\mathrm{d}S+\int_{\mathrm{s}-}t_{ij}^{\mathrm{s}-}\delta\varepsilon_{ij}\mathrm{d}S\\&=\int_0^L\int_0^{2\pi}\Big(N_{xx}\frac{\partial\delta u}{\partial x}+M_{xx}\frac{\partial\delta\varphi_x}{\partial x}+\frac{N_{\theta\theta}}{R}\Big(\frac{\partial\delta v}{\partial\theta}+\delta w\Big)+\frac{M_{\theta\theta}}{R}\frac{\partial\delta\varphi_\theta}{\partial\theta}\\&\quad+N_{x\theta}\Big(\frac{1}{R}\frac{\partial\delta u}{\partial\theta}+\frac{\partial\delta v}{\partial x}\Big)+M_{x\theta}\Big(\frac{1}{R}\frac{\partial\delta\varphi_x}{\partial\theta}+\frac{\partial\delta\varphi_\theta}{\partial x}\Big)+Q_x\Big(\delta\varphi_x+\frac{\partial\delta w}{\partial x}\Big)\\&\quad+Q_\theta\Big(\delta\varphi_\theta+\frac{1}{R}\frac{\partial\delta w}{\partial\theta}-\frac{\delta v}{R}\Big)+Q_x^{\mathrm{s}}\frac{\partial\delta w}{\partial x}+\frac{Q_\theta^{\mathrm{s}}}{R}\frac{\partial\delta w}{\partial\theta}\Big)R\mathrm{d}\theta\mathrm{d}x,\end{aligned}\quad(22)$$

in which the resultant forces and bending moments are defined as

$$\begin{cases}N_{xx}=\displaystyle\int_{-h/2}^{h/2}t_{xx}\mathrm{d}z+t_{xx}^{\mathrm{s}+}+t_{xx}^{\mathrm{s}-},\\N_{\theta\theta}=\displaystyle\int_{-h/2}^{h/2}t_{\theta\theta}\mathrm{d}z+t_{\theta\theta}^{\mathrm{s}+}+t_{\theta\theta}^{\mathrm{s}-},\\N_{x\theta}=\displaystyle\int_{-h/2}^{h/2}t_{x\theta}\mathrm{d}z+\frac{1}{2}(t_{x\theta}^{\mathrm{s}+}+t_{\theta x}^{\mathrm{s}+}+t_{x\theta}^{\mathrm{s}-}+t_{\theta x}^{\mathrm{s}-}),\end{cases}\quad(23)$$

$$\begin{cases}M_{xx}=\displaystyle\int_{-h/2}^{h/2}t_{xx}z\mathrm{d}z+\frac{h}{2}(t_{xx}^{\mathrm{s}+}-t_{xx}^{\mathrm{s}-}),\\M_{\theta\theta}=\displaystyle\int_{-h/2}^{h/2}t_{\theta\theta}z\mathrm{d}z+\frac{h}{2}(t_{\theta\theta}^{\mathrm{s}+}-t_{\theta\theta}^{\mathrm{s}-}),\\M_{x\theta}=\displaystyle\int_{-h/2}^{h/2}t_{x\theta}z\mathrm{d}z+\frac{h}{4}(t_{x\theta}^{\mathrm{s}+}+t_{\theta x}^{\mathrm{s}+}-t_{x\theta}^{\mathrm{s}-}-t_{\theta x}^{\mathrm{s}-}),\end{cases}\quad(24)$$

$$Q_x=\kappa\int_{-h/2}^{h/2}t_{xz}\mathrm{d}z,\quad Q_\theta=\kappa\int_{-h/2}^{h/2}t_{\theta z}\mathrm{d}z,\quad Q_x^{\mathrm{s}}=t_{xz}^{\mathrm{s}+}+t_{xz}^{\mathrm{s}-},\quad Q_\theta^{\mathrm{s}}=t_{\theta z}^{\mathrm{s}+}+t_{\theta z}^{\mathrm{s}-},\quad(25)$$

where κ is the shear correction factor. Similarly, the kinetic energy should also consider the bulk part as well as the two surface layers, which leads to

$$\begin{aligned}\delta K &= \int_V \rho(z)\frac{\partial u_i}{\partial t}\frac{\partial \delta u_i}{\partial t}\mathrm{d}V + \int_{\mathrm{s}+}\rho^{\mathrm{s}+}\frac{\partial u_i}{\partial t}\frac{\partial \delta u_i}{\partial t}\mathrm{d}S + \int_{\mathrm{s}-}\rho^{\mathrm{s}-}\frac{\partial u_i}{\partial t}\frac{\partial \delta u_i}{\partial t}\mathrm{d}S\\ &= \int_0^L\int_0^{2\pi}\Big(I_0\Big(\frac{\partial u}{\partial t}\frac{\partial \delta u}{\partial t}+\frac{\partial v}{\partial t}\frac{\partial \delta v}{\partial t}+\frac{\partial w}{\partial t}\frac{\partial \delta w}{\partial t}\Big)+I_1\Big(\frac{\partial \varphi_x}{\partial t}\frac{\partial \delta u}{\partial t}+\frac{\partial \varphi_\theta}{\partial t}\frac{\partial \delta v}{\partial t}\\ &\quad+\frac{\partial u}{\partial t}\frac{\partial \delta \varphi_x}{\partial t}+\frac{\partial v}{\partial t}\frac{\partial \delta \varphi_\theta}{\partial t}\Big)+I_2\Big(\frac{\partial \varphi_x}{\partial t}\frac{\partial \delta \varphi_x}{\partial t}+\frac{\partial \varphi_\theta}{\partial t}\frac{\partial \delta \varphi_\theta}{\partial t}\Big)\Big)R\mathrm{d}\theta\mathrm{d}x,\end{aligned}\tag{26}$$

where

$$\begin{cases} I_0 = \displaystyle\int_{-h/2}^{h/2}\rho(z)\mathrm{d}z+\rho^{\mathrm{s}+}+\rho^{\mathrm{s}-},\\ I_1 = \displaystyle\int_{-h/2}^{h/2}\rho(z)z\mathrm{d}z+\frac{h}{2}(\rho^{\mathrm{s}+}-\rho^{\mathrm{s}-}),\\ I_2 = \displaystyle\int_{-h/2}^{h/2}\rho(z)z^2\mathrm{d}z+\frac{h^2}{4}(\rho^{\mathrm{s}+}+\rho^{\mathrm{s}-}).\end{cases}\tag{27}$$

The first variation of the work done by external forces can be written as

$$\delta W = \int_0^L\int_0^{2\pi}(f_x\delta u+f_\theta\delta v+f_z\delta w)R\mathrm{d}\theta\mathrm{d}x,\tag{28}$$

where f_x, f_θ, and f_z are the distributed axial, circumferential, and radical forces, respectively.

Substituting Eqs. (22), (26), and (28) into Eq. (21) and integrating by parts, the equilibrium equations can be obtained as

$$\delta u:\ \frac{\partial N_{xx}}{\partial x}+\frac{1}{R}\frac{\partial N_{x\theta}}{\partial \theta}+f_x = I_0\frac{\partial^2 u}{\partial t^2}+I_1\frac{\partial^2 \varphi_x}{\partial t^2},\tag{29}$$

$$\delta v:\ \frac{\partial N_{x\theta}}{\partial x}+\frac{1}{R}\frac{\partial N_{\theta\theta}}{\partial \theta}+\frac{Q_\theta}{R}+f_\theta = I_0\frac{\partial^2 v}{\partial t^2}+I_1\frac{\partial^2 \varphi_\theta}{\partial t^2},\tag{30}$$

$$\delta w:\ \frac{\partial Q_x}{\partial x}+\frac{\partial Q_x^{\mathrm{s}}}{\partial x}+\frac{1}{R}\frac{\partial Q_\theta}{\partial \theta}+\frac{1}{R}\frac{\partial Q_\theta^{\mathrm{s}}}{\partial \theta}-\frac{N_{\theta\theta}}{R}+f_z = I_0\frac{\partial^2 w}{\partial t^2},\tag{31}$$

$$\delta \varphi_x:\ \frac{\partial M_{xx}}{\partial x}+\frac{1}{R}\frac{\partial M_{x\theta}}{\partial \theta}-Q_x = I_1\frac{\partial^2 u}{\partial t^2}+I_2\frac{\partial^2 \varphi_x}{\partial t^2},\tag{32}$$

$$\delta \varphi_\theta:\ \frac{\partial M_{x\theta}}{\partial x}+\frac{1}{R}\frac{\partial M_{\theta\theta}}{\partial \theta}-Q_\theta = I_1\frac{\partial^2 v}{\partial t^2}+I_2\frac{\partial^2 \varphi_\theta}{\partial t^2}.\tag{33}$$

The associated boundary conditions are given as follows:

$$\text{either}\quad u=0\quad\text{or}\quad N_{xx}n_x+N_{x\theta}n_\theta=0,\tag{34}$$

$$\text{either}\quad v=0\quad\text{or}\quad N_{x\theta}n_x+N_{\theta\theta}n_\theta=0,\tag{35}$$

$$\text{either}\quad w=0\quad\text{or}\quad (Q_x+Q_x^{\mathrm{s}})n_x+(Q_\theta+Q_\theta^{\mathrm{s}})n_\theta=0,\tag{36}$$

$$\text{either}\quad \varphi_x=0\quad\text{or}\quad M_{xx}n_x+M_{x\theta}n_\theta=0,\tag{37}$$

$$\text{either}\quad \varphi_\theta=0\quad\text{or}\quad M_{x\theta}n_x+M_{\theta\theta}n_\theta=0,\tag{38}$$

in which (n_x, n_θ) are the directional cosines of the outward unit normal to the boundary of the mid-plane.

2.4 Governing equations

By substituting Eqs. (10)–(20) into Eqs. (23)–(25) and integrating through the thickness, the stress resultants can be rewritten as

$$\begin{aligned}\big(1-(ea)^2\nabla^2\big)\,N_{xx} &= (1-l^2\nabla^2)\Big(A_1\frac{\partial u}{\partial x}+A_2\frac{\partial \varphi_x}{\partial x}+\frac{A_4}{R}\Big(\frac{\partial v}{\partial\theta}+w\Big)+\frac{A_5}{R}\frac{\partial\varphi_\theta}{\partial\theta}\\ &\quad+S_1\Big(\frac{\partial^2 w}{\partial x^2}+\frac{1}{R^2}\frac{\partial^2 w}{\partial\theta^2}\Big)-S_3\frac{\partial^2 w}{\partial t^2}+\tau^{\mathrm{s}+}+\tau^{\mathrm{s}-}\Big),\end{aligned}\tag{39}$$

$$\begin{aligned}\big(1-(ea)^2\nabla^2\big)\,N_{\theta\theta} &= (1-l^2\nabla^2)\Big(A_4\frac{\partial u}{\partial x}+A_5\frac{\partial \varphi_x}{\partial x}+\frac{A_1}{R}\Big(\frac{\partial v}{\partial\theta}+w\Big)+\frac{A_2}{R}\frac{\partial\varphi_\theta}{\partial\theta}\\ &\quad+S_1\Big(\frac{\partial^2 w}{\partial x^2}+\frac{1}{R^2}\frac{\partial^2 w}{\partial\theta^2}\Big)-S_3\frac{\partial^2 w}{\partial t^2}+\Big(1-\frac{w}{R}\Big)(\tau^{\mathrm{s}+}+\tau^{\mathrm{s}-})\Big),\end{aligned}\tag{40}$$

$$\big(1-(ea)^2\nabla^2\big)\,N_{x\theta} = (1-l^2\nabla^2)\Big(A_7\Big(\frac{1}{R}\frac{\partial u}{\partial\theta}+\frac{\partial v}{\partial x}\Big)+A_8\Big(\frac{1}{R}\frac{\partial\varphi_x}{\partial\theta}+\frac{\partial\varphi_\theta}{\partial x}\Big)\Big),\tag{41}$$

$$\begin{aligned}\big(1-(ea)^2\nabla^2\big)\,M_{xx} &= (1-l^2\nabla^2)\Big(A_2\frac{\partial u}{\partial x}+A_3\frac{\partial \varphi_x}{\partial x}+\frac{A_5}{R}\Big(\frac{\partial v}{\partial\theta}+w\Big)+\frac{A_6}{R}\frac{\partial\varphi_\theta}{\partial\theta}\\ &\quad+S_2\Big(\frac{\partial^2 w}{\partial x^2}+\frac{1}{R^2}\frac{\partial^2 w}{\partial\theta^2}\Big)-S_4\frac{\partial^2 w}{\partial t^2}+\frac{h}{2}(\tau^{\mathrm{s}+}-\tau^{\mathrm{s}-})\Big),\end{aligned}\tag{42}$$

$$\begin{aligned}\big(1-(ea)^2\nabla^2\big)\,M_{\theta\theta} &= (1-l^2\nabla^2)\Big(A_5\frac{\partial u}{\partial x}+A_6\frac{\partial \varphi_x}{\partial x}+\frac{A_2}{R}\Big(\frac{\partial v}{\partial\theta}+w\Big)+\frac{A_3}{R}\frac{\partial\varphi_\theta}{\partial\theta}\\ &\quad+S_2\Big(\frac{\partial^2 w}{\partial x^2}+\frac{1}{R^2}\frac{\partial^2 w}{\partial\theta^2}\Big)-S_4\frac{\partial^2 w}{\partial t^2}+\frac{h}{2}\Big(1-\frac{w}{R}\Big)(\tau^{\mathrm{s}+}-\tau^{\mathrm{s}-})\Big),\end{aligned}\tag{43}$$

$$\big(1-(ea)^2\nabla^2\big)\,M_{x\theta} = (1-l^2\nabla^2)\Big(A_8\Big(\frac{1}{R}\frac{\partial u}{\partial\theta}+\frac{\partial v}{\partial x}\Big)+A_9\Big(\frac{1}{R}\frac{\partial\varphi_x}{\partial\theta}+\frac{\partial\varphi_\theta}{\partial x}\Big)\Big),\tag{44}$$

$$\big(1-(ea)^2\nabla^2\big)\,Q_x = A_{10}(1-l^2\nabla^2)\Big(\varphi_x+\frac{\partial w}{\partial x}\Big),\tag{45}$$

$$\big(1-(ea)^2\nabla^2\big)\,Q_\theta = A_{10}(1-l^2\nabla^2)\Big(\varphi_\theta+\frac{1}{R}\frac{\partial w}{\partial\theta}-\frac{v}{R}\Big),\tag{46}$$

$$\big(1-(ea)^2\nabla^2\big)\,Q_x^{\mathrm{s}} = (\tau^{\mathrm{s}+}+\tau^{\mathrm{s}-})(1-l^2\nabla^2)\frac{\partial w}{\partial x},\tag{47}$$

$$\big(1-(ea)^2\nabla^2\big)\,Q_\theta^{\mathrm{s}} = (\tau^{\mathrm{s}+}+\tau^{\mathrm{s}-})(1-l^2\nabla^2)\frac{1}{R}\frac{\partial w}{\partial\theta},\tag{48}$$

where the coefficients $A_i\,(i=1,2,\cdots,10)$ and $S_j\,(j=1,2,\cdots,4)$ are given in Appendix A.

Employing Eqs. (39)–(48) into Eqs. (29)–(33), the governing equations in terms of displacements for vibration of the FG cylindrical nanoshells based on NSGT including surface effects are given by

$$\begin{aligned}&(1-l^2\nabla^2)\Big(A_1\frac{\partial^2 u}{\partial x^2}+\frac{A_7}{R^2}\frac{\partial^2 u}{\partial\theta^2}+A_2\frac{\partial^2\varphi_x}{\partial x^2}+\frac{A_8}{R^2}\frac{\partial^2\varphi_x}{\partial\theta^2}+\frac{A_4+A_7}{R}\frac{\partial^2 v}{\partial x\partial\theta}\\ &+\frac{A_5+A_8}{R}\frac{\partial^2\varphi_\theta}{\partial x\partial\theta}+\frac{A_4}{R}\frac{\partial w}{\partial x}+S_1\Big(\frac{\partial^3 w}{\partial x^3}+\frac{1}{R^2}\frac{\partial^3 w}{\partial x\partial\theta^2}\Big)-S_3\frac{\partial^3 w}{\partial x\partial t^2}\Big)\\ &=\big(1-(ea)^2\nabla^2\big)\Big(I_0\frac{\partial^2 u}{\partial t^2}+I_1\frac{\partial^2\varphi_x}{\partial t^2}\Big),\end{aligned}\tag{49}$$

$$(1-l^2\nabla^2)\Big(A_7\frac{\partial^2 v}{\partial x^2}+\frac{A_1}{R^2}\frac{\partial^2 v}{\partial\theta^2}+A_8\frac{\partial^2\varphi_\theta}{\partial x^2}+\frac{A_2}{R^2}\frac{\partial^2\varphi_\theta}{\partial\theta^2}+\frac{A_4+A_7}{R}\frac{\partial^2 u}{\partial x\partial\theta}+\frac{A_5+A_8}{R}\frac{\partial^2\varphi_x}{\partial x\partial\theta}$$
$$+\frac{A_{10}}{R}\varphi_\theta-\frac{A_{10}}{R^2}v+\frac{A_1+A_{10}-\tau^{s+}-\tau^{s-}}{R^2}\frac{\partial w}{\partial\theta}+\frac{S_1}{R}\frac{\partial^3 w}{\partial x^2\partial\theta}+\frac{S_1}{R^3}\frac{\partial^3 w}{\partial\theta^3}-\frac{S_3}{R}\frac{\partial^3 w}{\partial\theta\partial t^2}\Big)$$
$$=\big(1-(ea)^2\nabla^2\big)\Big(I_0\frac{\partial^2 v}{\partial t^2}+I_1\frac{\partial^2\varphi_\theta}{\partial t^2}\Big), \tag{50}$$

$$(1-l^2\nabla^2)\Big((A_{10}+\tau^{s+}+\tau^{s-})\Big(\frac{\partial^2 w}{\partial x^2}+\frac{1}{R^2}\frac{\partial^2 w}{\partial\theta^2}\Big)+\Big(A_{10}-\frac{A_5}{R}\Big)\frac{\partial\varphi_x}{\partial x}+\Big(\frac{A_{10}}{R}-\frac{A_2}{R^2}\Big)\frac{\partial\varphi_\theta}{\partial\theta}$$
$$-\frac{A_1+A_{10}}{R^2}\frac{\partial v}{\partial\theta}-\frac{A_4}{R}\frac{\partial u}{\partial x}-\frac{A_1-\tau^{s+}-\tau^{s-}}{R^2}w-\frac{S_1}{R}\frac{\partial^2 w}{\partial x^2}-\frac{S_1}{R^3}\frac{\partial^2 w}{\partial\theta^2}+\frac{S_3}{R}\frac{\partial^2 w}{\partial t^2}\Big)$$
$$=I_0\big(1-(ea)^2\nabla^2\big)\frac{\partial^2 w}{\partial t^2}, \tag{51}$$

$$(1-l^2\nabla^2)\Big(A_3\frac{\partial^2\varphi_x}{\partial x^2}+\frac{A_9}{R^2}\frac{\partial^2\varphi_x}{\partial\theta^2}+A_2\frac{\partial^2 u}{\partial x^2}+\frac{A_8}{R^2}\frac{\partial^2 u}{\partial\theta^2}+\frac{A_5+A_8}{R}\frac{\partial^2 v}{\partial x\partial\theta}+\frac{A_6+A_9}{R}\frac{\partial^2\varphi_\theta}{\partial x\partial\theta}$$
$$+\Big(\frac{A_5}{R}-A_{10}\Big)\frac{\partial w}{\partial x}-A_{10}\varphi_x+S_2\Big(\frac{\partial^3 w}{\partial x^3}+\frac{1}{R^2}\frac{\partial^3 w}{\partial x\partial\theta^2}\Big)-S_4\frac{\partial^3 w}{\partial x\partial t^2}\Big)$$
$$=\big(1-(ea)^2\nabla^2\big)\Big(I_1\frac{\partial^2 u}{\partial t^2}+I_2\frac{\partial^2\varphi_x}{\partial t^2}\Big), \tag{52}$$

$$(1-l^2\nabla^2)\Big(A_9\frac{\partial^2\varphi_\theta}{\partial x^2}+\frac{A_3}{R^2}\frac{\partial^2\varphi_\theta}{\partial\theta^2}+A_8\frac{\partial^2 v}{\partial x^2}+\frac{A_2}{R^2}\frac{\partial^2 v}{\partial\theta^2}+\frac{A_5+A_8}{R}\frac{\partial^2 u}{\partial x\partial\theta}$$
$$+\frac{A_6+A_9}{R}\frac{\partial^2\varphi_x}{\partial x\partial\theta}+\frac{S_2}{R}\frac{\partial^3 w}{\partial x^2\partial\theta}+\frac{S_2}{R^3}\frac{\partial^3 w}{\partial\theta^3}-\frac{S_4}{R}\frac{\partial^3 w}{\partial\theta\partial t^2}$$
$$+\Big(\frac{A_2}{R^2}-\frac{A_{10}}{R}-\frac{h}{2R^2}(\tau^{s+}-\tau^{s-})\Big)\frac{\partial w}{\partial\theta}+\frac{A_{10}}{R}v-A_{10}\varphi_\theta\Big)$$
$$=\big(1-(ea)^2\nabla^2\big)\Big(I_1\frac{\partial^2 v}{\partial t^2}+I_2\frac{\partial^2\varphi_\theta}{\partial t^2}\Big). \tag{53}$$

For homogenous cylindrical nanoshells, material properties are constants. Thus, we have $E(z)=E$, $\mu(z)=\mu$, $\rho(z)=\rho$, $\lambda^{s+}=\lambda^{s-}=\lambda^s$, $\mu^{s+}=\mu^{s-}=\mu^s$, $\tau^{s+}=\tau^{s-}=\tau^s$ and $\rho^{s+}=\rho^{s-}=\rho^s$. In this case, $A_2=A_5=A_8=S_1=S_3=I_1=0$, and Eqs. (49)–(53) can be simplified to

$$(1-l^2\nabla^2)\Big(A_1\frac{\partial^2 u}{\partial x^2}+\frac{A_7}{R^2}\frac{\partial^2 u}{\partial\theta^2}+\frac{A_4+A_7}{R}\frac{\partial^2 v}{\partial x\partial\theta}+\frac{A_4}{R}\frac{\partial w}{\partial x}\Big)=I_0\big(1-(ea)^2\nabla^2\big)\frac{\partial^2 u}{\partial t^2}, \tag{54}$$

$$(1-l^2\nabla^2)\Big(A_7\frac{\partial^2 v}{\partial x^2}+\frac{A_1}{R^2}\frac{\partial^2 v}{\partial\theta^2}+\frac{A_4+A_7}{R}\frac{\partial^2 u}{\partial x\partial\theta}-\frac{A_{10}}{R^2}v+\frac{A_{10}}{R}\varphi_\theta$$
$$+\frac{A_1+A_{10}-2\tau^s}{R^2}\frac{\partial w}{\partial\theta}\Big)=I_0\big(1-(ea)^2\nabla^2\big)\frac{\partial^2 v}{\partial t^2}, \tag{55}$$

$$(1-l^2\nabla^2)\Big((A_{10}+2\tau^s)\Big(\frac{\partial^2 w}{\partial x^2}+\frac{1}{R^2}\frac{\partial^2 w}{\partial\theta^2}\Big)+A_{10}\Big(\frac{\partial\varphi_x}{\partial x}+\frac{1}{R}\frac{\partial\varphi_\theta}{\partial\theta}\Big)-\frac{A_4}{R}\frac{\partial u}{\partial x}$$
$$-\frac{A_1+A_{10}}{R^2}\frac{\partial v}{\partial\theta}-\frac{A_1-2\tau^s}{R^2}w\Big)=I_0\big(1-(ea)^2\nabla^2\big)\frac{\partial^2 w}{\partial t^2}, \tag{56}$$

$$(1-l^2\nabla^2)\Big(A_3\frac{\partial^2\varphi_x}{\partial x^2}+\frac{A_9}{R^2}\frac{\partial^2\varphi_x}{\partial\theta^2}+\frac{A_6+A_9}{R}\frac{\partial^2\varphi_\theta}{\partial x\partial\theta}+S_2\Big(\frac{\partial^3 w}{\partial x^3}+\frac{1}{R^2}\frac{\partial^3 w}{\partial x\partial\theta^2}\Big)$$
$$-S_4\frac{\partial^3 w}{\partial x\partial t^2}-A_{10}\Big(\frac{\partial w}{\partial x}+\varphi_x\Big)\Big)=I_2\big(1-(ea)^2\nabla^2\big)\frac{\partial^2\varphi_x}{\partial t^2}, \tag{57}$$

$$(1-l^2\nabla^2)\Big(A_9\frac{\partial^2\varphi_\theta}{\partial x^2}+\frac{A_3}{R^2}\frac{\partial^2\varphi_\theta}{\partial\theta^2}+\frac{A_6+A_9}{R}\frac{\partial^2\varphi_x}{\partial x\partial\theta}+\frac{S_2}{R}\frac{\partial^3 w}{\partial x^2\partial\theta}+\frac{S_2}{R^3}\frac{\partial^3 w}{\partial\theta^3}$$
$$-\frac{S_4}{R}\frac{\partial^3 w}{\partial\theta\partial t^2}-A_{10}\Big(\varphi_\theta+\frac{1}{R}\frac{\partial w}{\partial\theta}-\frac{v}{R}\Big)\Big)=I_2\left(1-(ea)^2\nabla^2\right)\frac{\partial^2\varphi_\theta}{\partial t^2}. \tag{58}$$

It should be stated that by setting all the surface elastic constants to be zero, Eqs. (54)–(58) can be reduced to the governing equations of the nonlocal strain gradient shell model, which is identical to those of Mehralian et al.[61]. By taking the nonlocal and material length scale parameters to be zero, Eqs. (54)–(58) will be degenerated to the governing equations based on the surface elasticity theory, which is consistent with the formulation of Rouhi et al.[62].

3 Closed-form solutions for natural frequencies

In this section, closed-form solutions for natural frequencies of the FG cylindrical nanoshells under various boundary conditions are obtained through an analytical approach. Three typical types of boundary condition are considered, which are simply supported-simply supported (SS-SS), clamped-clamped (C-C), and clamped-simply supported (C-SS). In order to solve the governing equations, the displacement components are expressed as the following double Fourier series form[40–41]:

$$u(x,\theta,t)=\sum_{m=1}^{\infty}\sum_{n=1}^{\infty}U_{mn}\frac{\mathrm{d}X_m(x)}{\mathrm{d}x}\cos(n\theta)\exp(\mathrm{i}\omega_{mn}t), \tag{59}$$

$$v(x,\theta,t)=\sum_{m=1}^{\infty}\sum_{n=1}^{\infty}V_{mn}X_m(x)\sin(n\theta)\exp(\mathrm{i}\omega_{mn}t), \tag{60}$$

$$w(x,\theta,t)=\sum_{m=1}^{\infty}\sum_{n=1}^{\infty}W_{mn}X_m(x)\cos(n\theta)\exp(\mathrm{i}\omega_{mn}t), \tag{61}$$

$$\varphi_x(x,\theta,t)=\sum_{m=1}^{\infty}\sum_{n=1}^{\infty}\Phi_{xmn}\frac{\mathrm{d}X_m(x)}{\mathrm{d}x}\cos(n\theta)\exp(\mathrm{i}\omega_{mn}t), \tag{62}$$

$$\varphi_\theta(x,\theta,t)=\sum_{m=1}^{\infty}\sum_{n=1}^{\infty}\Phi_{\theta mn}X_m(x)\sin(n\theta)\exp(\mathrm{i}\omega_{mn}t), \tag{63}$$

where U_{mn}, V_{mn}, W_{mn}, Φ_{xmn}, and $\Phi_{\theta mn}$ are unknown constants, m and n are two positive integers denoting the wave numbers in the axial and circumferential directions, respectively, and $X_m(x)$ is the axial modal function. The explicit forms of $X_m(x)$ for different boundary conditions are given as follows[62–65]:

For the SS-SS boundary condition,

$$X_m(x)=\sin\frac{m\pi x}{L}. \tag{64}$$

For the C-C and C-SS boundary conditions,

$$X_m(x)=\cos\frac{a_m x}{L}-\cosh\frac{a_m x}{L}-\frac{\cos a_m-\cosh a_m}{\sin a_m-\sinh a_m}\Big(\sin\frac{a_m x}{L}-\sinh\frac{a_m x}{L}\Big), \tag{65}$$

where $a_1=4.73$, $a_2=7.853\ 2$, $a_3=10.995\ 6$, and $a_m=(m+0.5)\pi$ $(m\geqslant 4)$ for C-C boundary condition, and $a_1=3.926\ 6$, $a_2=7.068\ 6$, $a_3=10.210\ 2$, and $a_m=(m+0.25\pi)$ $(m\geqslant 4)$ for C-SS boundary condition.

For free vibration analysis, the external forces $f_x=f_\theta=f_z=0$. Substituting Eqs. (59)–(63) into Eqs. (49)–(53) and multiplying each equation by the corresponding eigenfunction, then

integrating along the length, we can obtain that

$$\left(\boldsymbol{K}_{5\times5}+\omega_{mn}^2\boldsymbol{M}_{5\times5}\right)\begin{pmatrix}U_{mn}\\V_{mn}\\W_{mn}\\\Phi_{xmn}\\\Phi_{\theta mn}\end{pmatrix}=\begin{pmatrix}0\\0\\0\\0\\0\end{pmatrix}, \tag{66}$$

where $\boldsymbol{K}_{5\times5}$ and $\boldsymbol{M}_{5\times5}$ are the stiffness matrix and the mass matrix, respectively. The elements of the two matrices are given in Appendix B. By setting the determinant of the coefficient matrix of Eq. (66) to be zero, the natural frequencies of FG cylindrical nanoshells can be obtained.

4 Comparative study

Before carrying out the numerical analyses, the validity of the present model and the accuracy of the analytical method are examined by comparing the degenerated results with those available in the literature. In Table 1, natural frequencies of an FG macroscale cylindrical shell with SS-SS boundary condition predicted by the present model (by ignoring all the size effects) are compared with those obtained by Loy et al.[59]. For comparison purpose, the inner surface of the FG cylindrical shell is assumed to be made of stainless steel with material properties: $E_{\rm m}$ = 207.788 GPa, $\mu_{\rm m}$ = 0.317 756, and $\rho_{\rm m}$ = 8 166 kg·m^{-3}, and the outer surface of the FG cylindrical shell is assumed to be made of Nickel with material properties: $E_{\rm c}$ = 205.098 GPa, $\mu_{\rm c}$ = 0.31, and $\rho_{\rm c}$ = 8 900 kg·m^{-3}. It is seen from Table 1 that the present results are in good agreement with the results of Loy et al.[59] for different circumferential wave numbers, power-law indices, and thickness-to-radius ratios.

Table 1 Comparisons of natural frequencies (Hz) of an FG macroscale cylindrical shell with SS-SS boundary condition ($m = 1$, $R = 1$ m, and $L/R = 20$)

n	$h/R = 0.002$						$h/R = 0.05$					
	$\xi = 0$		$\xi = 1$		$\xi = 2$		$\xi = 0$		$\xi = 1$		$\xi = 2$	
	Ref. [59]	Present	Ref. [59]	Present	Ref. [59]	Present	Ref. [59]	Present	Ref. [59]	Present	Ref. [59]	Present
1	12.894	12.894	13.211	13.211	13.321	13.321	12.917	12.917	13.234	13.234	13.344	13.344
2	4.369 0	4.369 0	4.474 2	4.474 2	4.511 4	4.511 5	31.603	31.552	32.418	32.372	32.683	32.637
3	4.048 9	4.048 8	4.148 6	4.148 6	4.182 7	4.182 7	88.267	87.922	90.569	90.239	91.309	90.976
4	6.857 7	6.857 6	7.033 0	7.033 0	7.090 5	7.090 6	168.99	167.80	173.41	172.23	174.83	173.63
5	10.955	10.954	11.238	11.238	11.329	11.329	273.14	270.10	280.28	277.23	282.57	279.49
6	16.037	16.037	16.453	16.453	16.587	16.587	400.56	394.15	411.03	404.56	414.39	407.85
7	22.061	22.060	22.633	22.633	22.454	22.818	551.22	539.28	565.63	553.51	570.25	558.02
8	29.017	29.015	29.770	29.769	30.014	30.013	725.08	704.76	744.04	723.34	750.13	729.22
9	36.902	36.900	37.861	37.859	38.171	38.169	922.15	889.81	946.27	913.24	954.0	920.65
10	45.716	45.713	46.904	46.902	47.288	47.285	1 142.4	1 093.6	1 172.3	1 122.3	1 181.9	1 131.4

To examine the accuracy of the present analytical method for more complex boundary conditions, Table 2 compares the dimensionless natural frequencies of a homogenous macroscale cylindrical shell, under SS-SS, C-SS, and C-C boundary conditions, obtained by the present analytical method with those obtained by Loy et al.[66] using generalized differential quadrature (GDQ) method and Zhang et al.[67] through wave propagation approach. One can find that for the three types of boundary conditions considered, the present analytical solutions agree well with the results obtained by the GDQ method and the wave propagation method.

As the third example, a comparative study is performed to verify the accuracy of the present model in capturing size effects. For this objective, Table 3 tabulates the dimensionless natural frequencies of a homogenous nanoscale cylindrical shell with SS-SS and C-C boundary conditions predicted by the present work and Ghorbani et al.[58]. Results are presented for different values of nonlocal parameter and material length scale parameter with and without surface effects. Material properties are taken as: $E = 210$ GPa, $\rho = 2\ 331\ \mathrm{kg{\cdot}m^{-3}}$, $\mu = 0.24$, $\lambda_{\mathrm{s}} = -4.488\ \mathrm{N{\cdot}m^{-1}}$, $\mu_{\mathrm{s}} = -2.774\ \mathrm{N{\cdot}m^{-1}}$, $\tau_{\mathrm{s}} = 0.605\ \mathrm{N{\cdot}m^{-1}}$ and $\rho_{\mathrm{s}} = 3.17 \times 10^{-7}\ \mathrm{kg{\cdot}m^{-3}}$. It can be seen from Table 3 that the present results have a good consistency with those of Ghorbani et al.[58] for both SS-SS and C-C boundary conditions. From the above comparisons, the reliability of the present model and analytical method are well-validated.

Table 2 Comparisons of dimensionless natural frequencies ($\omega R\sqrt{\rho(1-\mu^2)/E}$) of a homogeneous macroscale cylindrical shell under different boundary conditions ($m = 1$, $L/R = 20$, $h/R = 0.01$, and $\mu = 0.3$)

n	SS-SS			C-C			C-SS		
	Ref. [66]	Ref. [67]	Present	Ref. [66]	Ref. [67]	Present	Ref. [66]	Ref. [67]	Present
1	0.016 101	0.016 101	0.016 102	0.032 885	0.034 879	0.034 395	0.023 974	0.024 721	0.024 831
2	0.009 382	0.009 382	0.009 387	0.013 932	0.014 052	0.014 263	0.011 225	0.011 281	0.011 369
3	0.022 105	0.022 105	0.022 105	0.022 672	0.022 725	0.022 716	0.022 310	0.022 335	0.022 325
4	0.042 095	0.042 095	0.042 085	0.042 208	0.042 271	0.042 208	0.042 139	0.042 166	0.042 133
5	0.068 008	0.068 008	0.067 978	0.068 046	0.068 116	0.068 023	0.068 024	0.068 054	0.067 999
6	0.099 730	0.099 731	0.099 665	0.099 748	0.099 823	0.099 691	0.099 738	0.099 771	0.099 680
7	0.137 239	0.137 240	0.137 117	0.137 249	0.137 328	0.137 137	0.137 244	0.137 279	0.137 130
8	0.180 527	0.180 527	0.180 317	0.180 535	0.180 617	0.180 336	0.180 531	0.180 569	0.180 329
9	0.229 594	0.229 596	0.229 254	0.229 599	0.229 684	0.229 272	0.229 596	0.229 636	0.229 266
10	0.284 435	0.284 438	0.283 916	0.284 439	0.284 526	0.283 934	0.284 437	0.284 478	0.283 928

Table 3 Comparisons of dimensionless natural frequencies ($\omega R\sqrt{\rho/E}$) of a homogeneous nanoscale cylindrical shell with C-C and SS-SS boundary conditions ($h = 0.3$ nm, $R = 10h$, $L = 20R$, and $m = n = 1$)

$((ea), l)$	C-C				SS-SS			
	With surface effects		Without surface effect		With surface effects		Without surface effect	
	Ref. [58]	Present	Ref. [58]	Present	Ref. [58]	Present	Ref. [58]	Present
(0, 0)	0.074 945	0.075 190	0.034 699	0.035 944	0.072 410	0.072 410	0.017 016	0.017 016
($50h$, 0)	0.014 497	0.014 528	0.006 712	0.006 945	0.014 035	0.014 035	0.003 298	0.003 298
(0,$10h$)	0.106 870	0.107 222	0.050 013	0.051 382	0.103 033	0.103 033	0.024 213	0.024 213
($50h$,$10h$)	0.020 683	0.020 716	0.009 678	0.009 928	0.019 971	0.019 971	0.004 693	0.004 693

5 Results and discussion

In this section, based on the proposed size-dependent shell model, the effects of nonlocal parameter, material length scale parameter, power-law index, radius-to-thickness ratio, length-to-radius ratio, and surface effects on the free vibration behavior of FG cylindrical nanoshells with different boundary conditions (SS-SS, C-SS, and C-C) are investigated. The ceramic and metal constituents are selected as Silicon and Aluminum, respectively. Material properties of Silicon and Aluminum are given in Table 4. In the numerical analyses, the thickness of the FG cylindrical nanoshell is considered as $h = 1$ nm, axial wave number is fixed at $m = 1$, and the shear correction factor is taken as $\kappa = 5/6$.

Table 4 Material properties of silicon and aluminum[55,68]

Silicon	E_c/GPa	μ_c	$\rho_c/(\mathrm{kg\cdot m^{-3}})$	$\mu^{s+}/(\mathrm{N\cdot m^{-1}})$	$\lambda^{s+}/(\mathrm{N\cdot m^{-1}})$	$\tau^{s+}/(\mathrm{N\cdot m^{-1}})$	$\rho^{s+}/(\mathrm{kg\cdot m^{-3}})$
	210	0.24	2 331	−2.774	−4.488	0.604 8	3.17×10^{-7}
Aluminum	E_m/GPa	μ_m	$\rho_m/(\mathrm{kg\cdot m^{-3}})$	$\mu^{s-}/(\mathrm{N\cdot m^{-1}})$	$\lambda^{s-}/(\mathrm{N\cdot m^{-1}})$	$\tau^{s-}/(\mathrm{N\cdot m^{-1}})$	$\rho^{s-}/(\mathrm{kg\cdot m^{-3}})$
	68.5	0.35	2 700	−0.376	6.842	0.910 8	5.46×10^{-7}

To illustrate the numerical results and to highlight the size effects, the dimensionless natural frequency ϖ_{mn} and frequency ratio are defined as

$$\varpi_{mn} = 100\omega_{mn}h\sqrt{\frac{\rho_c}{E_c}}, \tag{67}$$

$$\text{Frequency ratio} = \frac{\varpi_{mn} \text{ predicted by NSGT with/without surface effects}}{\varpi_{mn} \text{ predicted by classical continuum theory}}. \tag{68}$$

Note that the results of the classical continuum theory can be acquired from the present model by setting the two scale parameters and all the surface elastic constants to be zero.

5.1 Benchmark results

Tables 5–7 illustrate the dimensionless natural frequencies of an FG cylindrical nanoshell based on the NSGT without surface effects for SS-SS, C-SS, and C-C boundary conditions, respectively. The geometric parameters are taken as: $R/h = 10$ and $L/R = 5$. Results are presented for different values of normalized nonlocal parameter ($(ea)/h$), normalized material length scale parameter (l/h), circumferential wave number (n) and power-law index (ξ). Note that when $\xi = 0$, the nanoshell is made of pure silicon, and the inner and outer surface have the same surface material properties. It can be seen from Tables 5–7 that an increase in the nonlocal parameter or power-law index leads to a decrease in the natural frequency; conversely, an increase in the strain gradient parameter results in an increase in the natural frequency. Moreover, with the increase in the circumferential wave number, the natural frequencies first decrease and then increase. In particular, the fundamental frequency always occurs at $n = 2$. On the other hand, we can find that for the three types of boundary condition considered, the natural frequencies associated with the C-SS boundary condition are higher than those of the SS-SS boundary condition, but lower than those of C-C boundary condition, which indicates that stiffer boundary condition produces higher natural frequencies. The corresponding dimensionless natural frequencies of the FG cylindrical nanoshell based on NSGT with surface effects for different boundary conditions are tabulated in Tables 8–10. Comparing the results with surface effects with those without surface effects, it can be found that surface effects may affect the circumferential wave number at which the fundamental frequency occurs. For instance, when ignoring surface effects, the fundamental frequency of the SS-SS FG cylindrical nanoshell with $\xi = 1$ and $(ea) = 0$ occurs at $n = 2$. However, by taking surface effects into account, the fundamental frequency occurs at $n = 1$. Moreover, the results tabulated in Tables 5–10 can be used as benchmarks for prospective researchers to compare their results.

5.2 Coupling effect of nonlocal parameter and material length scale parameter

To explore the coupling effect of nonlocal parameter and material length scale parameter on the vibrational behavior of FG cylindrical nanoshell under different boundary conditions, Fig. 2 plots the variations of the frequency ratio as a function of the scale parameter ratio ($l/(ea)$) for SS-SS, C-SS, and C-C boundary conditions, when $R/h = 10$, $L/R = 2$, $\xi = 1$, and $n = 3$. Surface effects are neglected in this example. It is seen that, for SS-SS boundary condition (see Fig. 2(a)), when the nonlocal parameter is smaller than the material length scale parameter ($l/(ea) < 1$), the FG cylindrical nanoshell exhibits a stiffness-softening behavior, leading to the natural frequencies predicted by NSGT always lower than those of classical continuum theory. When the nonlocal parameter is larger than the material length scale parameter ($l/(ea) > 1$),

Table 5 Dimensionless natural frequencies of FG cylindrical nanoshells without surface effects under SS-SS boundary condition

$(ea)/h$	n	$\xi=0$			$\xi=1$			$\xi=2$		
		$l/h=0$	$l/h=2$	$l/h=4$	$l/h=0$	$l/h=2$	$l/h=4$	$l/h=0$	$l/h=2$	$l/h=4$
0	1	1.966 4	2.020 5	2.174 7	1.536 0	1.578 2	1.698 7	1.381 6	1.419 6	1.528 0
	2	1.190 6	1.291 0	1.553 8	0.896 3	0.971 8	1.169 7	0.816 0	0.884 8	1.064 9
	3	2.355 4	2.762 7	3.726 5	1.762 7	2.067 5	2.788 8	1.623 3	1.904 1	2.568 3
	4	4.320 2	5.559 1	8.223 3	3.240 1	4.169 3	6.167 4	2.984 8	3.840 8	5.681 4
	5	6.818 4	9.680 7	15.342 4	5.117 6	7.265 9	11.515 4	4.711 6	6.689 4	10.601 7
2	1	1.913 7	1.966 4	2.116 5	1.494 8	1.536 0	1.653 3	1.344 6	1.381 6	1.487 1
	2	1.098 0	1.190 6	1.433 0	0.826 5	0.896 3	1.078 7	0.752 5	0.816 0	0.982 1
	3	2.008 1	2.355 4	3.177 1	1.502 8	1.762 7	2.377 6	1.384 0	1.623 3	2.189 7
	4	3.357 4	4.320 2	6.390 6	2.518 0	3.240 1	4.792 9	2.319 6	2.984 8	4.415 3
	5	4.802 4	6.818 4	10.806 2	3.604 5	5.117 6	8.110 6	3.318 5	4.711 6	7.467 1
4	1	1.778 0	1.826 9	1.966 4	1.388 8	1.427 0	1.536 0	1.249 2	1.283 6	1.381 6
	2	0.912 3	0.989 3	1.190 6	0.686 8	0.744 7	0.896 3	0.625 2	0.678 0	0.816 0
	3	1.488 7	1.746 2	2.355 4	1.114 1	1.306 8	1.762 7	1.026 0	1.203 5	1.623 3
	4	2.269 6	2.920 5	4.320 2	1.702 2	2.190 4	3.240 1	1.568 1	2.017 8	2.984 8
	5	3.030 2	4.302 3	6.818 4	2.274 3	3.229 1	5.117 6	2.093 9	2.972 9	4.711 6

Table 6 Dimensionless natural frequencies of FG cylindrical nanoshells without surface effects under C-SS boundary condition

$(ea)/h$	n	$\xi=0$			$\xi=1$			$\xi=2$		
		$l/h=0$	$l/h=2$	$l/h=4$	$l/h=0$	$l/h=2$	$l/h=4$	$l/h=0$	$l/h=2$	$l/h=4$
0	1	2.491 4	2.574 8	2.809 6	1.939 7	2.004 8	2.188 2	1.743 1	1.801 7	1.966 7
	2	1.457 7	1.585 2	1.917 2	1.108 1	1.204 9	1.457 0	1.0054	1.093 2	1.321 9
	3	2.417 8	2.840 1	3.837 7	1.811 0	2.127 2	2.874 1	1.666 5	1.957 4	2.644 7
	4	4.348 0	5.600 6	8.291 8	3.260 8	4.200 2	6.218 4	3.003 6	3.868 8	5.727 8
	5	6.839 1	9.717 6	15.408 0	5.132 9	7.293 2	11.563 9	4.725 5	6.714 4	10.646 1
2	1	2.421 3	2.502 3	2.730 5	1.885 1	1.948 4	2.126 6	1.694 1	1.751 1	1.911 4
	2	1.342 8	1.460 2	1.766 0	1.020 7	1.109 9	1.342 1	0.926 1	1.007 0	1.217 6
	3	2.059 3	2.419 0	3.268 6	1.542 5	1.811 8	2.448 0	1.419 4	1.667 2	2.252 6
	4	3.376 3	4.349 0	6.438 7	2.532 1	3.261 5	4.828 6	2.332 3	3.004 2	4.447 7
	5	4.813 8	6.839 9	10.845 3	3.612 9	5.133 5	8.139 5	3.326 1	4.726 0	7.493 5
4	1	2.241 8	2.316 8	2.528 1	1.745 5	1.804 1	1.969 1	1.568 7	1.621 4	1.769 8
	2	1.113 4	1.210 7	1.464 3	0.846 4	0.920 3	1.112 8	0.767 9	0.835 0	1.009 6
	3	1.524 9	1.791 3	2.420 4	1.142 2	1.341 6	1.812 7	1.051 1	1.234 5	1.668 1
	4	2.280 9	2.938 0	4.349 8	1.710 6	2.203 4	3.262 1	1.575 6	2.029 6	3.004 7
	5	3.036 2	4.314 1	6.840 4	2.278 8	3.237 8	5.133 8	2.097 9	2.980 9	4.726 4

Table 7 Dimensionless natural frequencies of FG cylindrical nanoshells without surface effects under C-C boundary condition

$(ea)/h$	n	$\xi=0$			$\xi=1$			$\xi=2$		
		$l/h=0$	$l/h=2$	$l/h=4$	$l/h=0$	$l/h=2$	$l/h=4$	$l/h=0$	$l/h=2$	$l/h=4$
0	1	2.805 1	2.935 9	3.294 0	2.174 5	2.276 6	2.556 1	1.951 6	2.043 5	2.294 9
	2	1.710 1	1.872 3	2.289 6	1.304 5	1.428 3	1.746 8	1.180 5	1.292 5	1.580 6
	3	2.491 8	2.932 8	3.971 9	1.869 3	2.199 8	2.978 7	1.718 3	2.022 1	2.738 0
	4	4.374 4	5.640 1	8.356 7	3.281 2	4.230 3	6.267 7	3.021 9	3.896 0	5.772 3
	5	6.854 1	9.744 8	15.456 8	5.144 2	7.313 7	11.600 5	4.735 8	6.733 0	10.679 4
2	1	2.724 4	2.851 5	3.199 2	2.112 0	2.211 2	2.482 6	1.895 6	1.984 8	2.229 0
	2	1.574 3	1.723 6	2.107 8	1.200 9	1.314 9	1.608 1	1.086 8	1.189 9	1.455 1
	3	2.121 3	2.496 7	3.381 3	1.591 4	1.872 7	2.535 8	1.462 9	1.721 4	2.330 9
	4	3.395 4	4.377 9	6.486 6	2.546 9	3.283 6	4.865 1	2.345 6	3.024 1	4.480 6
	5	4.822 9	6.856 9	10.876 1	3.619 7	5.146 3	8.162 6	3.332 3	4.737 7	7.514 6
4	1	2.518 7	2.636 1	2.957 3	1.952 7	2.044 4	2.295 2	1.752 7	1.835 1	2.060 7
	2	1.304 0	1.427 6	1.745 8	0.994 8	1.089 2	1.332 0	0.900 2	0.985 6	1.205 3
	3	1.569 9	1.847 7	2.502 4	1.177 8	1.386 0	1.876 7	1.082 6	1.274 0	1.725 0
	4	2.293 1	2.956 6	4.380 7	1.720 1	2.217 6	3.285 6	1.584 1	2.042 4	3.026 0
	5	3.041 3	4.324 0	6.858 6	2.282 6	3.245 3	5.147 5	2.101 4	2.987 6	4.738 8

Table 8 Dimensionless natural frequencies of FG cylindrical nanoshells with surface effects under SS-SS boundary condition

$(ea)/h$	n	$\xi=0$			$\xi=1$			$\xi=2$		
		$l/h=0$	$l/h=2$	$l/h=4$	$l/h=0$	$l/h=2$	$l/h=4$	$l/h=0$	$l/h=2$	$l/h=4$
0	1	1.757 7	1.806 1	1.944 0	1.407 7	1.446 5	1.556 9	1.284 2	1.319 6	1.420 3
	2	1.571 6	1.704 2	2.051 1	1.498 3	1.624 7	1.955 5	1.456 6	1.579 5	1.901 1
	3	2.644 8	3.102 4	4.185 7	2.525 2	2.962 3	3.997 3	2.449 7	2.873 8	3.878 0
	4	4.200 4	5.406 4	8.003 5	3.902 0	5.023 3	7.440 9	3.752 1	4.830 4	7.155 6
	5	6.139 9	8.722 8	13.850 2	5.576 5	7.926 4	12.604 7	5.323 8	7.567 5	12.036 0
2	1	1.710 7	1.757 7	1.891 9	1.370 0	1.407 7	1.515 2	1.249 9	1.284 2	1.382 3
	2	1.449 3	1.571 6	1.891 6	1.381 7	1.498 3	1.803 3	1.343 3	1.456 6	1.753 2
	3	2.254 7	2.644 8	3.568 0	2.152 6	2.525 2	3.407 1	2.088 3	2.449 7	3.305 4
	4	3.263 8	4.200 4	6.216 3	3.031 6	3.902 0	5.776 8	2.915 0	3.752 1	5.555 1
	5	4.323 2	6.139 9	9.739 8	3.925 5	5.576 5	8.852 7	3.747 5	5.323 8	8.452 2
4	1	1.589 3	1.633 0	1.757 7	1.272 9	1.307 9	1.407 7	1.161 2	1.193 2	1.284 2
	2	1.204 2	1.305 8	1.571 6	1.148 0	1.244 9	1.498 3	1.116 1	1.210 2	1.456 6
	3	1.671 4	1.960 5	2.644 8	1.595 7	1.871 8	2.525 2	1.548 0	1.815 8	2.449 7
	4	2.206 1	2.839 0	4.200 4	2.048 9	2.636 8	3.902 0	1.970 2	2.535 5	3.752 1
	5	2.727 3	3.872 7	6.139 9	2.476 1	3.516 3	5.576 5	2.363 8	3.356 8	5.323 8

Table 9 Dimensionless natural frequencies of FG cylindrical nanoshells with surface effects under C-SS boundary condition

$(ea)/h$	n	$\xi=0$			$\xi=1$			$\xi=2$		
		$l/h=0$	$l/h=2$	$l/h=4$	$l/h=0$	$l/h=2$	$l/h=4$	$l/h=0$	$l/h=2$	$l/h=4$
0	1	2.193 8	2.266 8	2.472 4	1.726 5	1.784 0	1.945 9	1.565 5	1.617 6	1.764 3
	2	1.732 6	1.883 0	2.275 2	1.603 2	1.741 7	2.103 3	1.546 0	1.679 5	2.027 9
	3	2.687 3	3.156 5	4.265 5	2.553 2	2.998 8	4.052 5	2.474 4	2.906 2	3.927 3
	4	4.221 3	5.438 7	8.058 0	3.916 6	5.046 9	7.481 7	3.765 3	4.852 0	7.193 2
	5	6.155 8	8.752 0	13.903 0	5.588 1	7.948 8	12.646 2	5.334 5	7.588 3	12.074 5
2	1	2.132 0	2.202 9	2.402 7	1.677 9	1.733 8	1.891 2	1.521 5	1.572 1	1.714 7
	2	1.595 9	1.734 4	2.095 7	1.476 8	1.604 4	1.937 4	1.424 1	1.547 0	1.868 0
	3	2.288 7	2.688 3	3.632 5	2.174 5	2.553 8	3.450 8	2.107 3	2.474 9	3.344 1
	4	3.277 4	4.222 1	6.253 6	3.040 5	3.917 2	5.803 8	2.923 0	3.765 8	5.579 8
	5	4.331 5	6.156 4	9.770 5	3.931 1	5.588 6	8.875 9	3.752 6	5.334 9	8.473 6
4	1	1.974 0	2.039 6	2.224 6	1.553 7	1.605 4	1.751 1	1.408 8	1.455 7	1.587 7
	2	1.323 2	1.438 1	1.737 6	1.224 4	1.330 2	1.606 3	1.180 8	1.282 7	1.548 8
	3	1.694 7	1.990 5	2.689 4	1.610 0	1.890 8	2.554 6	1.560 3	1.832 4	2.475 6
	4	2.213 9	2.851 8	4.222 8	2.053 6	2.645 3	3.917 6	1.974 2	2.543 1	3.766 3
	5	2.731 5	3.881 6	6.156 8	2.478 7	3.522 6	5.588 9	2.366 0	3.362 5	5.335 2

Table 10 Dimensionless natural frequencies of FG cylindrical nanoshells with surface effects under C-C boundary condition

$(ea)/h$	n	$\xi=0$			$\xi=1$			$\xi=2$		
		$l/h=0$	$l/h=2$	$l/h=4$	$l/h=0$	$l/h=2$	$l/h=4$	$l/h=0$	$l/h=2$	$l/h=4$
0	1	2.457 8	2.570 8	2.880 7	1.910 6	1.998 6	2.240 2	1.726 1	1.805 5	2.023 4
	2	1.895 7	2.070 1	2.521 3	1.708 8	1.863 6	2.264 9	1.635 4	1.783 0	2.165 9
	3	2.736 5	3.219 2	4.357 9	2.585 7	3.040 6	4.114 7	2.502 4	2.942 5	3.981 8
	4	4.240 8	5.468 3	8.107 6	3.930 3	5.068 1	7.517 8	3.777 5	4.871 1	7.225 9
	5	6.167 2	8.773 2	13.941 5	5.596 6	7.964 9	12.675 8	5.342 1	7.603 1	12.101 8
2	1	2.387 1	2.496 9	2.797 7	1.855 7	1.941 2	2.175 8	1.676 6	1.753 7	1.965 3
	2	1.745 1	1.905 7	2.321 0	1.573 1	1.715 6	2.085 0	1.505 5	1.641 4	1.993 8
	3	2.329 5	2.740 3	3.709 4	2.201 0	2.588 1	3.502 0	2.130 1	2.504 6	3.388 8
	4	3.291 2	4.243 5	6.289 6	3.049 9	3.932 1	5.829 5	2.931 3	3.779 2	5.602 9
	5	4.338 2	6.169 4	9.794 3	3.935 8	5.598 1	8.893 8	3.756 7	5.343 6	8.489 9
4	1	2.206 8	2.308 2	2.586 1	1.715 8	1.794 8	2.011 6	1.550 2	1.621 5	1.817 0
	2	1.445 5	1.578 4	1.922 3	1.303 0	1.421 0	1.726 9	1.247 1	1.359 6	1.651 5
	3	1.723 9	2.027 8	2.744 7	1.628 7	1.915 1	2.591 0	1.576 2	1.853 3	2.507 2
	4	2.222 4	2.865 2	4.245 7	2.059 3	2.654 6	3.933 7	1.979 2	2.551 3	3.780 6
	5	2.735 2	3.889 0	6.170 6	2.481 1	3.527 9	5.599 1	2.368 2	3.367 4	5.344 4

the FG cylindrical nanoshell exerts a stiffness-hardening behavior, resulting in the natural frequencies of NSGT always higher than those of classical continuum theory. In particular, when the two scale parameters are equal ($l/(ea)=1$), the results of NSGT reduce to those of classical continuum theory. These observations have been reported by many researchers[13,14,69–70]. Nevertheless, for C-SS and C-C boundary conditions (see Figs. 2(b) and 2(c)), it is interesting to see that, when $l/(ea)<1$, the results of NSGT can be lower or higher than or even equal to those of classical continuum theory by taking a specific scale parameter ratio, which is quite

different than the case of SS-SS boundary condition. More interestingly, when $l/(ea) = 1$, unlike the SS-SS FG cylindrical nanoshells whose natural frequencies obtained by NSGT are identical to those of classical continuum theory, the natural frequencies of C-SS and C-C FG cylindrical nanoshells evaluated using NSGT are higher than the results of classical continuum theory. In other words, under C-SS and C-C boundary conditions, the predictions of NSGT cannot reduce to those of classical continuum theory when the nonlocal parameter equals to the material length scale parameter. From this observations, we can conclude that the coupling effect of nonlocal stress and strain gradient on the vibrational behavior of FG nanoshells depends not only on the relative magnitude of the two scale parameters but also on the boundary condition. Therefore, it is of great importance to take different boundary conditions into account when studying the mechanical behaviors of nanostructures with the framework of NSGT.

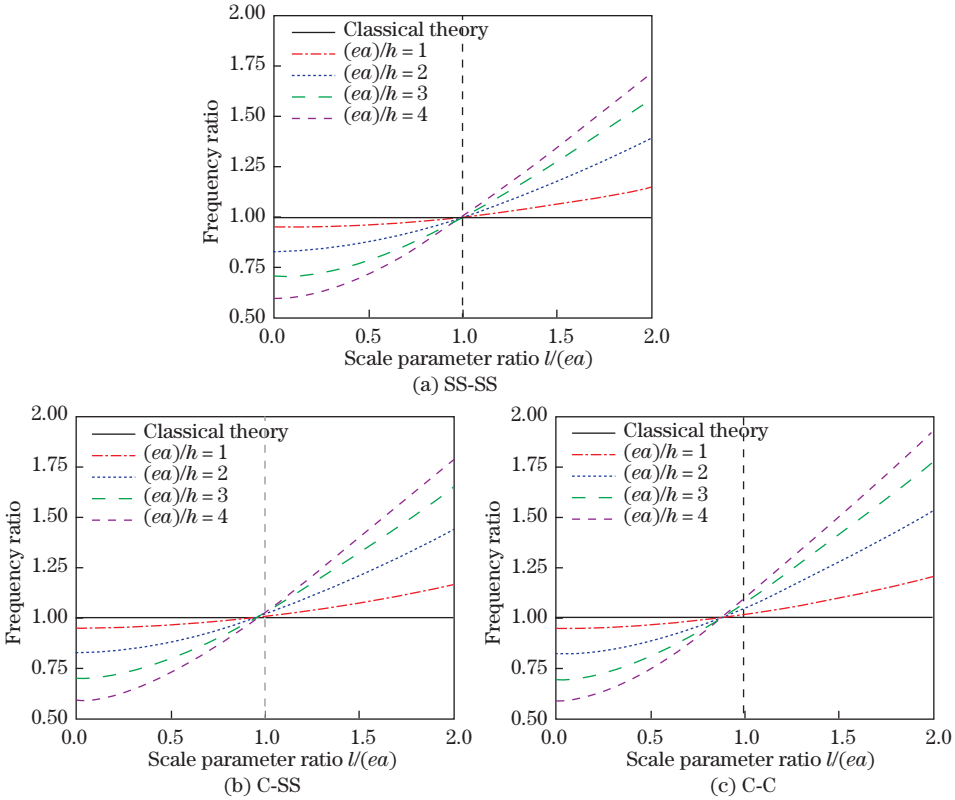

Fig. 2 Variation of frequency ratio with respect to scale parameter ratio for different values of normalized nonlocal parameter (color online)

5.3 Effect of power-law index

The effect of power-law index on the frequency ratio of FG cylindrical nanoshell under different boundary conditions is shown in Figs. 3 and 4 for various normalized nonlocal parameters and material length scale parameters, respectively. Parameters $R/h = 10$, $L/R = 5$ and $n = 2$ are taken in this example. It is observed from Figs. 3 and 4 that when surface effects are not included, for different values of scale parameters, the frequency ratios are nearly unchanged as the power-law index increases from 0 to 10. This implies that nonlocal effect and strain gradient effect on the vibration of FG cylindrical nanoshells are not sensitive to the change in the power-law index. However, for the case of including surface effects, it can be seen that increasing the power-law index leads to an increase in the frequency ratio. In other words, surface effects on the vibration behavior of FG cylindrical nanoshell becomes more and more

important as the increase in the power-law index. In addition, comparing the results of SS-SS, C-SS and C-C boundary conditions, it is clearly seen that surface effects play a more important role in the vibration of FG cylindrical shells with SS-SS boundary condition.

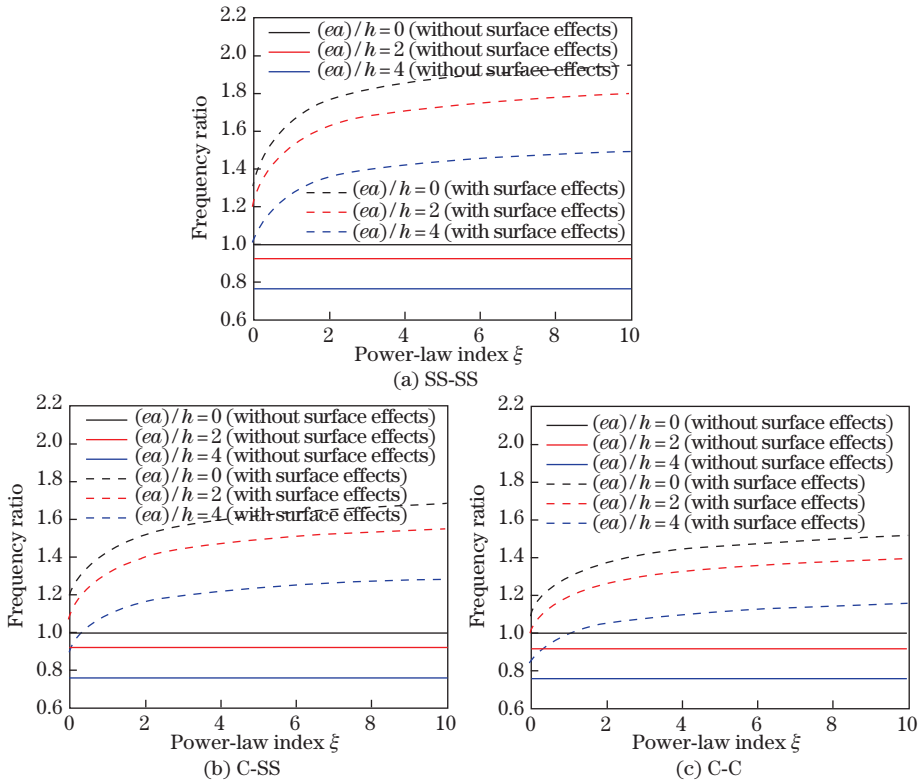

Fig. 3 Variation of frequency ratio with respect to power-law index for different values of normalized nonlocal parameter ($l/h = 0$) (color online)

5.4 Effect of radius-to-thickness ratio

The effect of radius-to-thickness ratio on the frequency ratio of FG cylindrical nanoshell with SS-SS, C-SS, and C-C boundary conditions is depicted in Figs. 5 and 6 for different values of normalized nonlocal parameter and material length scale parameter, respectively. Results are obtained with $L/R = 10$, $\xi = 1$ and $n = 2$. It is seen that when surface effects are not considered, the frequency ratios associated with different nonlocal parameters or material length scale parameters all approach to 1 as the radius-to-thickness ratio increases from 5 to 25, which means that nonlocal effect and strain gradient effect gradually decrease with the increase in radius-to-thickness ratio. When accounting for surface effects, one can observe that the gaps between the frequency ratios with surface effects and those without surface effects are getting wider as the radius-to-thickness ratio increases, revealing that increasing the radius-to-thickness ratio will increase surface effects, and this trend is more remarkable for SS-SS boundary condition. Besides, it can be concluded from Figs. 5 and 6 that, at higher values of radius-to-thickness ratio, surface effects play a dominant role in the vibration of FG cylindrical nanoshells, and nonlocal and strain gradient effects are less important in this situation.

5.5 Effect of length-to-radius ratio

Figures 7 and 8 illustrate the variations of frequency ratio with respect to the length-to-radius ratio for various normalized nonlocal parameters and material length scale parameters, respectively. Same as Figs. 5 and 6, results are presented for SS-SS, C-SS, and C-C FG

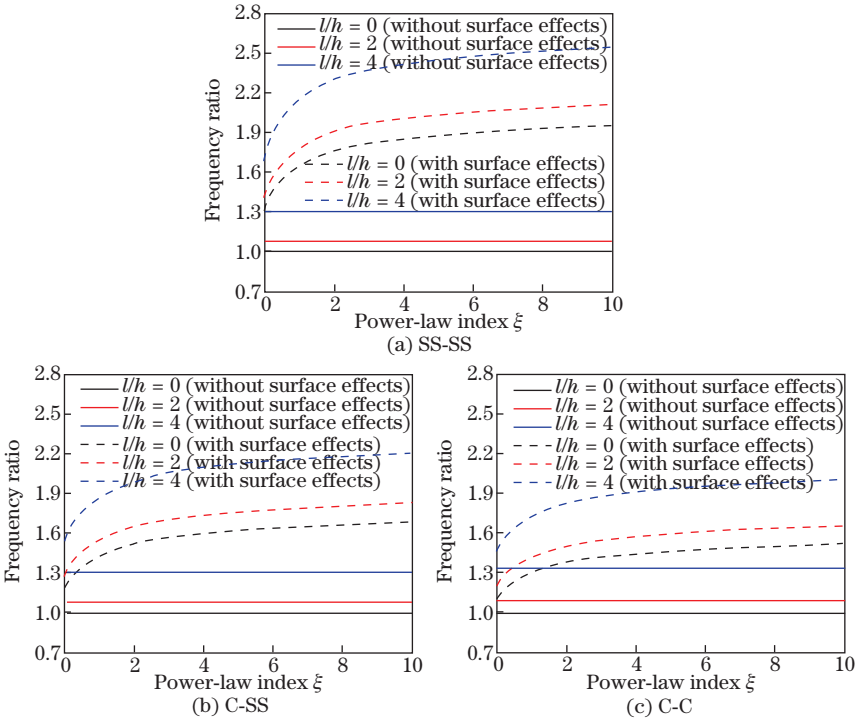

Fig. 4 Variation of frequency ratio with respect to power-law index for different values of normalized material length scale parameter ($(ea)/h = 0$) (color online)

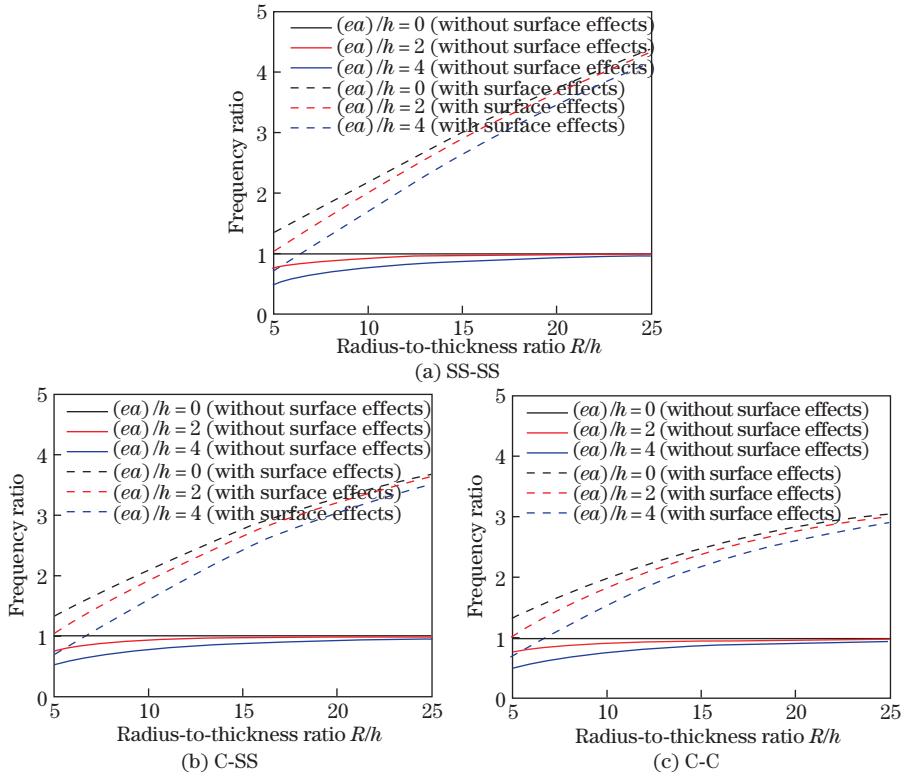

Fig. 5 Variation of frequency ratio with respect to radius-to-thickness ratio for different values of normalized nonlocal parameter ($l/h = 0$) (color online)

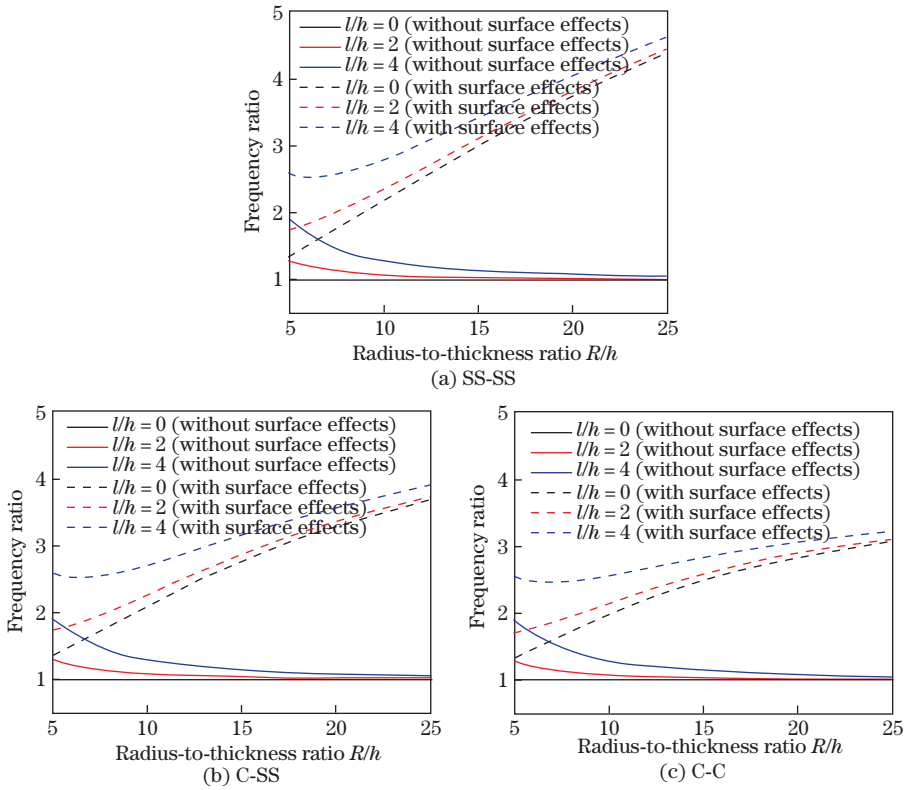

Fig. 6 Variation of frequency ratio with respect to radius-to-thickness ratio for different values of normalized material length scale parameter ($(ea)/h = 0$) (color online)

cylindrical nanoshells with or without surface effects. Parameters $R/h = 5$, $\xi = 1$ and $n = 1$ are selected in this example. It is observed that without considering surface effects, the frequency ratios corresponding to different scale parameters gradually reduce with the increase in length-to-radius ratio for all three boundary conditions, which implies that increasing the length-to-radius ratio results in the decrease in nonlocal effect and strain gradient effect on the vibrational behavior of FG cylindrical nanoshell, but compared with surface effects, nonlocal effect and strain gradient effects are not sensitive to the change in length-to-radius ratio. Under the influence of surface effects, it can be seen from Figs. 7 and 8 that as the length-to-radius ratio increases, the frequency ratios with surface effects are first lower than then higher than those without surface effects. That is to say, surface effects tend to decrease the natural frequencies of short nanoshells, but increase the natural frequencies of long nanoshells. Moreover, it is found that, at higher values of length-to-radius ratio, surface effects play a more important role than nonlocal effect and strain gradient effect in the vibration of FG cylindrical nanoshells, and similar to the case of Figs. 5 and 6, this phenomenon is more notable for SS-SS boundary condition.

6 Conclusions

In the present work, a size-dependent FG cylindrical shell model is developed within

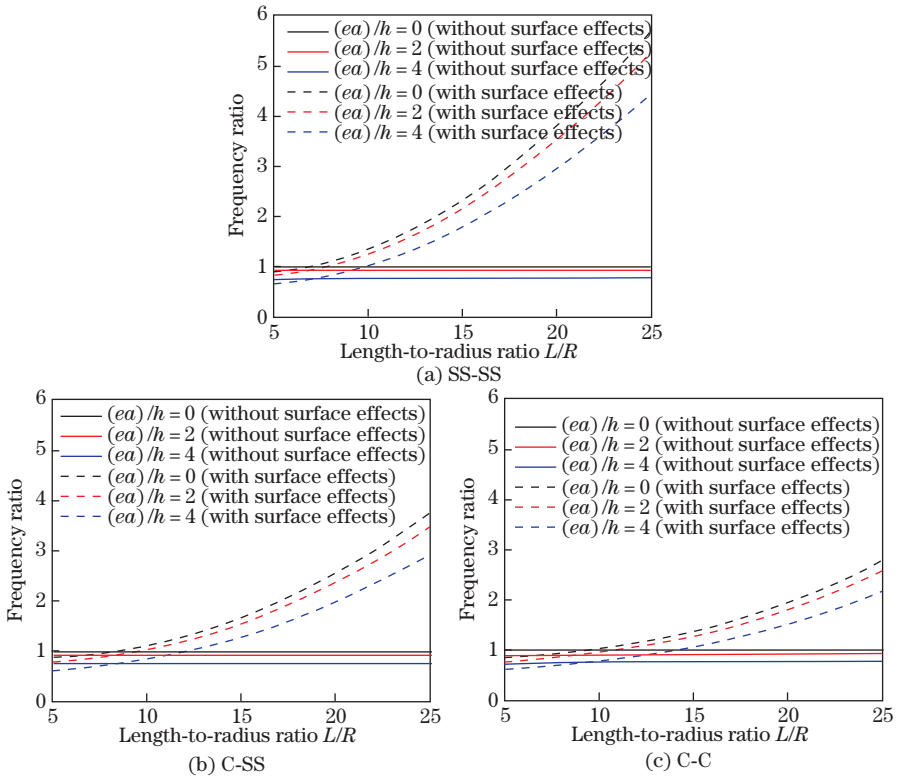

Fig. 7 Variation of frequency ratio with respect to length-to-radius ratio for different values of normalized nonlocal parameter ($l/h = 0$) (color online)

the framework of NSGT and surface elasticity theory. By adopting the proposed model, the influences of nonlocal parameter, material length scale parameter, power-law index, radius-to-thickness ratio, length-to-radius ratio and surface effects on the free vibration of FG cylindrical nanoshells under SS-SS, C-SS and C-C boundary conditions are investigated. From the numerical results, the following main conclusions can be drawn:

(i) The coupling effect of nonlocal parameter and material length scale parameter on the vibration of FG cylindrical nanoshells depends not only on the relative magnitude of the two scale parameters but also on the boundary condition. In particular, when the two scale parameters are equal, the predictions of NSGT reduce to those of the classical continuum theory for SS-SS boundary condition. However, the results of NSGT are higher than those of the classical continuum theory for C-SS and C-C boundary conditions.

(ii) Nonlocal effect and strain gradient effect on the vibration of FG cylindrical nanoshells are not sensitive to the change in power-law index, while surface effects on the vibration of FG cylindrical nanoshells becomes more and more important with the increase in the power-law index.

(iii) Increasing the radius-to-thickness ratio or length-to-radius ratio will decrease nonlocal effect and strain gradient effect on the vibration of FG cylindrical nanoshells, whereas increase surface effects on the vibration of FG cylindrical nanoshells.

(iv) Surface effects play a more important role than nonlocal effect and strain gradient effect in the vibration of FG cylindrical nanoshells with higher values of radius-to-thickness ratio and length-to-radius ratio, and this situation is more significant for SS-SS boundary condition.

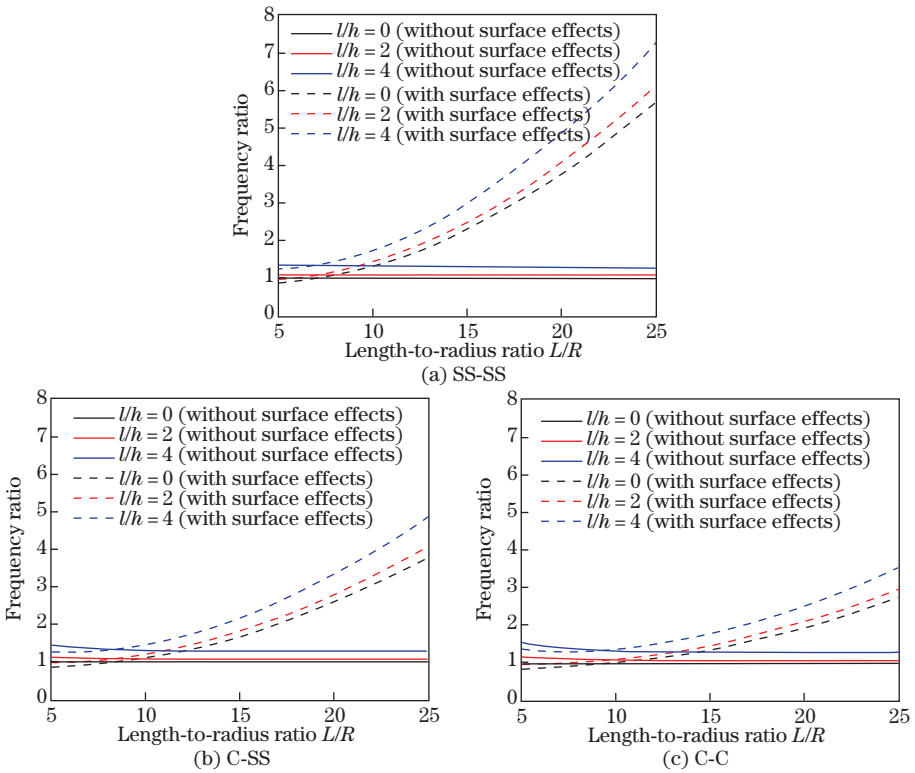

Fig. 8 Variation of frequency ratio with respect to length-to-radius ratio for different values of normalized material length scale parameter ($(ea)/h = 0$) (color online)

References

[1] ERINGEN, A. C. Nonlocal polar elastic continua. *International Journal of Engineering Science*, **10**, 1–16 (1972)

[2] ERINGEN, A. C. On differential equations of nonlocal elasticity and solutions of screw dislocation and surface waves. *Journal of Applied Physics*, **54**(9), 4703–4710 (1983)

[3] MINDLIN, R. D. Micro-structure in linear elasticity. *Archive for Rational Mechanics and Analysis*, **16**, 51–78 (1964)

[4] MINDLIN, R. D. Second gradient of strain and surface-tension in linear elasticity. *International Journal of Solids Structures*, **1**, 417–438 (1965)

[5] AIFANTIS, E. C. On the role of gradients in the localization of deformation and fracture. *International Journal of Engineering Science*, **30**, 1279–1299 (1992)

[6] LAM, D., YANG, F., CHONG, A., WANG, J., and TONG, P. Experiments and theory in strain gradient elasticity. *Journal of the Mechanics and Physics of Solids*, **51**, 1477–1508 (2003)

[7] GURTIN, M. E. and MURDOCH, A. I. A continuum theory of elastic material surfaces. *Archive for Rational Mechanics and Analysis*, **57**, 291–323 (1975)

[8] GURTIN, M. E. and MURDOCH, A. I. Surface stress in solids. *International Journal of Solids and Structures*, **14**, 431–440 (1978)

[9] ELTAHER, M. A., KHATER, M. E., and EMAM, S. A. A review on nonlocal elastic models for bending, buckling, vibrations, and wave propagation of nanoscale beams. *Applied Mathematical Modelling*, **40**, 4109–4128 (2016)

[10] THAI, H. T., VO, T. P., NGUYEN, T. K., and KIM, S. E. A review of continuum mechanics models for size-dependent analysis of beams and plates. *Composite Structures*, **177**, 196–219 (2017)

[11] GHAYESH, M. H. and FARAJPOUR, A. A review on the mechanics of functionally graded nanoscale and microscale structures. *International Journal of Engineering Science*, **137**, 8–36 (2019)

[12] LIM, C. W., ZHANG, G., and REDDY, J. N. A higher-order nonlocal elasticity and strain gradient theory and its applications in wave propagation. *Journal of the Mechanics and Physics of Solids*, **78**, 298–313 (2015)

[13] LI, L., LI, X., and HU, Y. Free vibration analysis of nonlocal strain gradient beams made of functionally graded material. *International Journal of Engineering Science*, **102**, 77–92 (2016)

[14] SIMSEK, M. Nonlinear free vibration of a functionally graded nanobeam using nonlocal strain gradient theory and a novel Hamiltonian approach. *International Journal of Engineering Science*, **105**, 12–27 (2016)

[15] LI, X., LI, L., HU, Y., DING, Z., and DENG, W. Bending, buckling and vibration of axially functionally graded beams based on nonlocal strain gradient theory. *Composite Structures*, **165**, 250–265 (2017)

[16] HADI, A., NEJAD, M. Z., and HOSSEINI, M. Vibrations of three-dimensionally graded nanobeams. *International Journal of Engineering Science*, **128**, 12–23 (2018)

[17] TANG, Y. G., LIU, Y., and ZHAO, D. Effects of neutral surface deviation on nonlinear resonance of embedded temperature-dependent functionally graded nanobeams. *Composite Structures*, **184**, 969–979 (2018)

[18] SHE, G. L., REN, Y. R., YUAN, F. G., and XIAO, W. S. On vibrations of porous nanotubes. *International Journal of Engineering Science*, **125**, 23–35 (2018)

[19] VAHIDI-MOGHADDAM, A., RAJAEI, A., VATANKHAH, R., and HAIRI-YAZDI, M. R. Terminal sliding mode control with non-symmetric input saturation for vibration suppression of electrostatically actuated nanobeams in the presence of Casimir force. *Applied Mathematical Modelling*, **60**, 416–434 (2018)

[20] LI, L. and HU, Y. Post-buckling analysis of functionally graded nanobeams incorporating nonlocal stress and microstructure-dependent strain gradient effects. *International Journal of Mechanical Sciences*, **120**, 159–170 (2017)

[21] LIU, H., LV, Z., and WU, H. Nonlinear free vibration of geometrically imperfect functionally graded sandwich nanobeams based on nonlocal strain gradient theory. *Composite Structures*, **214**, 47–61 (2019)

[22] AL-SHUJAIRI, M. and MOLLAMAHMUTOĞLU, C. Buckling and free vibration analysis of functionally graded sandwich microbeams resting on elastic foundation by using nonlocal strain gradient theory in conjunction with higher order shear theories under thermal effect. *Composites Part B*, **154**, 292–312 (2018)

[23] APUZZO, A., BARRETTA, R., FAGHIDIAN, S. A., LUCIANO, R., and MAROTTI DE SCIARRA, F. Nonlocal strain gradient exact solutions for functionally graded inflected nano-beams. *Composites Part B*, **164**, 667–674 (2019)

[24] TANG, H., LI, L., and HU, Y. Coupling effect of thickness and shear deformation on size-dependent bending of micro/nano-scale porous beams. *Applied Mathematical Modelling*, **66**, 527–547 (2019)

[25] BARATI, M. R. A general nonlocal stress-strain gradient theory for forced vibration analysis of heterogeneous porous nanoplates. *European Journal of Mechanics A/Solids*, **67**, 215–230 (2018)

[26] EBRAHIMI, F., BARATI, M. R., and DABBAGH, A. A nonlocal strain gradient theory for wave propagation analysis in temperature-dependent inhomogeneous nanoplates. *International Journal of Engineering Science*, **107**, 169–182 (2016)

[27] AREF, M., KIANI, M., and RABCZUK, T. Application of nonlocal strain gradient theory to size dependent bending analysis of a sandwich porous nanoplate integrated with piezomagnetic face-sheets. *Composites Part B*, **168**, 320–333 (2019)

[28] MAHINZARE, M., ALIPOUR, M. J., SADATSAKKAK, S. A., and GHADIRI, M. A nonlocal strain gradient theory for dynamic modeling of a rotary thermo piezo electrically actuated nano FG circular plate. *Mechanical Systems and Signal Processing*, **115**, 323–337 (2019)

[29] MIRJAVADI, S. S., AFSHARI, B. M., BARATI, M. R., and HAMOUDA, A. M. S. Transient response of porous FG nanoplates subjected to various pulse loads based on nonlocal stress-strain gradient theory. *European Journal of Mechanics A/Solids*, **74**, 210–220 (2019)

[30] RADIC, N. On buckling of porous double-layered FG nanoplates in the Pasternak elastic foundation based on nonlocal strain gradient elasticity. *Composites Part B*, **153**, 465–479 (2018)

[31] KARAMI, B., SHAHSAVARI, D., and LI, L. Temperature-dependent flexural wave propagation in nanoplate-type porous heterogenous material subjected to in-plane magnetic field. *Journal of Thermal Stresses*, **41**, 483–499 (2018)

[32] SHAHVERDI, H. and BARATI, M. R. Vibration analysis of porous functionally graded nanoplates. *International Journal of Engineering Science*, **120**, 82–99 (2017)

[33] SAHMANI, S. and AGHDAM, M. M. Nonlinear instability of axially loaded functionally graded multilayer graphene platelet-reinforced nanoshells based on nonlocal strain gradient elasticity theory. *International Journal of Mechanical Sciences*, **131/132**, 95–106 (2017)

[34] SAHMANI, S. and AGHDAM, M. M. A nonlocal strain gradient hyperbolic shear deformable shell model for radial postbuckling analysis of functionally graded multilayer GPLRC nanoshells. *Composite Structures*, **178**, 97–109 (2017)

[35] SAHMANI, S. and FATTAHI, A. M. Small scale effects on buckling and postbuckling behaviors of axially loaded FGM nanoshells based on nonlocal strain gradient elasticity theory. *Applied Mathematics and Mechanics* (*English Edition*), **39**(4), 561–580 (2018) https://doi.org/10.1007/s10483-018-2312-8

[36] SAHMANI, S. and AGHDAM, M. M. Nonlocal strain gradient shell model for axial buckling and postbuckling analysis of magneto-electro-elastic composite nanoshells. *Composites Part B*, **132**, 258–274 (2018)

[37] KARAMI, B., SHAHSAVARI, D., JANGHORBAN, M., DIMITRI, R., and TORNABENE, F. Wave propagation of porous nanoshells. *Nanomaterials*, **9**, 1–19 (2019)

[38] SHE, G. L., YUAN, F. G., and REN, Y. R. On wave propagation of porous nanotubes. *International Journal of Engineering Science*, **130**, 62–74 (2018)

[39] SOBHY, M. and ZENKOUR, A. M. Porosity and inhomogeneity effects on the buckling and vibration of double-FGM nanoplates via a quasi-3D refined theory. *Composite Structures*, **220**, 289–303 (2019)

[40] BARATI, M. R. Vibration analysis of porous FG nanoshells with even and uneven porosity distributions using nonlocal strain gradient elasticity. *Acta Mechanica*, **229**(3), 1183–1196 (2018)

[41] FALEH, N. M., AHMED, R. A., and FENJAN, R. M. On vibrations of porous FG nanoshells. *International Journal of Engineering Science*, **133**, 1–14 (2018)

[42] MA, L. H., KE, L. L., REDDY, J. N., YANG, J., KITIPORNCHAI, S., and WANG, Y. S. Wave propagation characteristics in magneto-electro-elastic nanoshells using nonlocal strain gradient theory. *Composite Structures*, **199**, 10–23 (2018)

[43] ANSARI, R., ASHRAFI, M. A., POURASHRAF, T., and SAHMANI, S. Vibration and buckling characteristics of functionally graded nanoplates subjected to thermal loading based on surface elasticity theory. *Acta Astronautica*, **109**, 42–51 (2015)

[44] ANSARI, R. and NOROUZZADEH, A. Nonlocal and surface effects on the buckling behavior of functionally graded nanoplates: An isogeometric analysis. *Physica E*, **84**, 84–97 (2016)

[45] AREFI, M. Surface effect and non-local elasticity in wave propagation of functionally graded piezoelectric nano-rod excited to applied voltage. *Applied Mathematics and Mechanics* (*English Edition*), **37**(3), 289–302 (2016) https://doi.org/10.1007/s10483-016-2039-6

[46] ATTIA, M. A. On the mechanics of functionally graded nanobeams with the account of surface elasticity. *International Journal of Engineering Science*, **115**, 73–101 (2017)

[47] HOSSEINI-HASHEMI, S., NAHAS, I., FAKHER, M., and NAZEMNEZHAD, R. Surface effects on free vibration of piezoelectric functionally graded nanobeams using nonlocal elasticity. *Acta Mechanica*, **225**, 1555–1564 (2014)

[48] HOSSEINI-HASHEMI, S., NAZEMNEZHAD, R., and BEDROUD, M. Surface effects on nonlinear free vibration of functionally graded nanobeams using nonlocal elasticity. *Applied Mathematical Modelling*, **38**, 3538–3553 (2014)

[49] LÜ, C. F., LIM, C. W., and CHEN, W. Q. Size-dependent elastic behavior of FGM ultra-thin films based on generalized refined theory. *International Journal of Solids and Structures*, **46**, 1176–1185 (2009)

[50] SHAAT, M., MAHMOUD, F. F., ALSHORBAGY, A. E., and ALIELDIN, S. S. Bending analysis of ultra-thin functionally graded Mindlin plates incorporating surface energy effects. *International Journal of Mechanical Sciences*, **75**, 223–232 (2013)

[51] SHANAB, R. A., ATTIA, M. A., and MOHAMED, S. A. Nonlinear analysis of functionally graded nanoscale beams incorporating the surface energy and microstructure effects. *International Journal of Mechanical Sciences*, **131/132**, 908–923 (2017)

[52] WANG, Y. Q., WAN, Y. H., and ZU, J. W. Nonlinear dynamic characteristics of functionally graded sandwich thin nanoshells conveying fluid incorporating surface stress influence. *Thin-Walled Structures*, **135**, 537–547 (2019)

[53] ZHU, C. S., FANG, X. Q., and LIU, J. X. Surface energy effect on buckling behavior of the functionally graded nano-shell covered with piezoelectric nano-layers under torque. *International Journal of Mechanical Sciences*, **133**, 662–673 (2017)

[54] NOROUZZADEH, A. and ANSARI, R. Isogeometric vibration analysis of functionally graded nanoplates with the consideration of nonlocal and surface effects. *Thin-Walled Structures*, **127**, 354–372 (2018)

[55] ATTIA, M. A. and ABDEL-RAHMAN, A. A. On vibrations of functionally graded viscoelastic nanobeams with surface effects. *International Journal of Engineering Science*, **127**, 1–32 (2018)

[56] LU, L., GUO, X. M., and ZHAO, J. On the mechanics of Kirchhoff and Mindlin plates incorporating surface energy. *International Journal of Engineering Science*, **124**, 24–40 (2018)

[57] LU, L., GUO, X., and ZHAO, J. A unified size-dependent plate model based on nonlocal strain gradient theory including surface effects. *Applied Mathematical Modelling*, **68**, 583–602 (2019)

[58] GHORBANI, K., MOHAMMADI, K., RAJABPOUR, A., and GHADIRI, M. Surface and size-dependent effects on the free vibration analysis of cylindrical shell based on Gurtin-Murdoch and nonlocal strain gradient theories. *Journal of Physics and Chemistry of Solids*, **129**, 140–150 (2019)

[59] LOY, C. T., LAM, K. Y., and REDDY, J. N. Vibration of functionally graded cylindrical shells. *International Journal of Mechanical Sciences*, **41**, 309–324 (1999)

[60] LU, P., HE, L. H., LEE, H. P., and LU, C. Thin plate theory including surface effects. *International Journal of Solids and Structures*, **46**, 4631–4647 (2006)

[61] MEHRALIAN, F., BENI, Y. T., and ZEVERDEJANI, M. K. Nonlocal strain gradient theory calibration using molecular dynamics simulation based on small scale vibration of nanotubes. *Physica B*, **514**, 61–69 (2017)

[62] ROUHI, H., ANSARI, R., and DARVIZEH, M. Size-dependent free vibration analysis of nanoshells based on the surface stress elasticity. *Applied Mathematical Modelling*, **40**, 3128–3140 (2016)

[63] LOY, C. T. and LAM, K. Y. Vibration of cylindrical shells with ring support. *International Journal of Mechanical Sciences*, **39**(4), 445–471 (1997)

[64] LEE, H. M. and KWAK, M. K. Free vibration analysis of a circular cylindrical shell using the Rayleigh-Ritz method and comparison of different shell theories. *Journal of Sound and Vibration*, **353**, 344–377 (2015)

[65] LI, X., DU, C. C., and LI, Y. H. Parametric resonance of an FG cylindrical thin shell with periodic rotating angular speeds in thermal environment. *Applied Mathematical Modelling*, **59**, 393–409 (2018)

[66] LOY, C. T., LAM, K. Y., and SHU, C. Analysis of cylindrical shells using generalized differential quadrature. *Shock and Vibration*, **4**(3), 193–198 (1997)

[67] ZHANG, X. M., LIU, G. R., and LAM, K. Y. Vibration analysis of thin cylindrical shells using wave propagation approach. *Journal of Sound and Vibration*, **239**(3), 397–403 (2001)

[68] ANSARI, R. and GHOLAMI, R. Surface effect on the large amplitude periodic forced vibration of first-order shear deformable rectangular nanoplates with various edge supports. *Acta Astronautica*, **118**, 72–89 (2016)

[69] LU, L., GUO, X. M., and ZHAO, J. Size-dependent vibration analysis of nanobeams based on the nonlocal strain gradient theory. *International Journal of Engineering Science*, **116**, 12–24 (2017)

[70] LU, L., GUO, X. M., and ZHAO, J. A unified nonlocal strain gradient model for nanobeams and the importance of higher order terms. *International Journal of Engineering Science*, **119**, 265–277 (2017)

Appendix A

Coefficients appearing in Eqs. (39)–(48) are listed as follows:

$$A_1=\int_{-h/2}^{h/2}\frac{E(z)}{1-\mu(z)^2}\mathrm{d}z+\lambda^{\mathrm{s}+}+2\mu^{\mathrm{s}+}+\lambda^{\mathrm{s}-}+2\mu^{\mathrm{s}-},\tag{A1}$$

$$A_2=\int_{-h/2}^{h/2}\frac{E(z)}{1-\mu(z)^2}z\mathrm{d}z+\frac{h}{2}(\lambda^{\mathrm{s}+}+2\mu^{\mathrm{s}+}-\lambda^{\mathrm{s}-}-2\mu^{\mathrm{s}-}),\tag{A2}$$

$$A_3=\int_{-h/2}^{h/2}\frac{E(z)}{1-\mu(z)^2}z^2\mathrm{d}z+\frac{h^2}{4}(\lambda^{\mathrm{s}+}+2\mu^{\mathrm{s}+}+\lambda^{\mathrm{s}-}+2\mu^{\mathrm{s}-}),\tag{A3}$$

$$A_4=\int_{-h/2}^{h/2}\frac{\mu(z)E(z)}{1-\mu(z)^2}\mathrm{d}z+\lambda^{\mathrm{s}+}+\tau^{\mathrm{s}+}+\lambda^{\mathrm{s}-}+\tau^{\mathrm{s}-},\tag{A4}$$

$$A_5=\int_{-h/2}^{h/2}\frac{\mu(z)E(z)}{1-\mu(z)^2}z\mathrm{d}z+\frac{h}{2}(\lambda^{\mathrm{s}+}+\tau^{\mathrm{s}+}-\lambda^{\mathrm{s}-}-\tau^{\mathrm{s}-}),\tag{A5}$$

$$A_6=\int_{-h/2}^{h/2}\frac{\mu(z)E(z)}{1-\mu(z)^2}z^2\mathrm{d}z+\frac{h^2}{4}(\lambda^{\mathrm{s}+}+\tau^{\mathrm{s}+}+\lambda^{\mathrm{s}-}+\tau^{\mathrm{s}-}),\tag{A6}$$

$$A_7=\int_{-h/2}^{h/2}\frac{E(z)}{2(1+\mu(z))}\mathrm{d}z+\frac{1}{2}(2\mu^{\mathrm{s}+}-\tau^{\mathrm{s}+}+2\mu^{\mathrm{s}-}-\tau^{\mathrm{s}-}),\tag{A7}$$

$$A_8=\int_{-h/2}^{h/2}\frac{E(z)}{2(1+\mu(z))}z\mathrm{d}z+\frac{h}{4}(2\mu^{\mathrm{s}+}-\tau^{\mathrm{s}+}-2\mu^{\mathrm{s}-}+\tau^{\mathrm{s}-}),\tag{A8}$$

$$A_9=\int_{-h/2}^{h/2}\frac{E(z)}{2(1+\mu(z))}z^2\mathrm{d}z+\frac{h^2}{8}(2\mu^{\mathrm{s}+}-\tau^{\mathrm{s}+}+2\mu^{\mathrm{s}-}-\tau^{\mathrm{s}-}),\tag{A9}$$

$$A_{10}=\kappa\int_{-h/2}^{h/2}\frac{E(z)}{2(1+\mu(z))}\mathrm{d}z,\tag{A10}$$

$$S_1=\int_{-h/2}^{h/2}\frac{\mu(z)}{1-\mu(z)}\Big(\frac{1}{2}(\tau^{s+}-\tau^{s-})+\frac{z}{h}(\tau^{s+}+\tau^{s-})\Big)\mathrm{d}z, \tag{A11}$$

$$S_2=\int_{-h/2}^{h/2}\frac{\mu(z)}{1-\mu(z)}\Big(\frac{1}{2}(\tau^{s+}-\tau^{s-})+\frac{z}{h}(\tau^{s+}+\tau^{s-})\Big)z\mathrm{d}z, \tag{A12}$$

$$S_3=\int_{-h/2}^{h/2}\frac{\mu(z)}{1-\mu(z)}\Big(\frac{1}{2}(\rho^{s+}-\rho^{s-})+\frac{z}{h}(\rho^{s+}+\rho^{s-})\Big)\mathrm{d}z, \tag{A13}$$

$$S_4=\int_{-h/2}^{h/2}\frac{\mu(z)}{1-\mu(z)}\Big(\frac{1}{2}(\rho^{s+}-\rho^{s-})+\frac{z}{h}(\rho^{s+}+\rho^{s-})\Big)z\mathrm{d}z. \tag{A14}$$

Appendix B

Elements of the coefficient matrix of Eq. (66) are listed as follows:

$$\begin{cases}
K_{11}=A_1e_3-A_7b_n^2e_1,\quad K_{12}=(A_4+A_7)b_ne_1,\quad K_{13}=\Big(\dfrac{A_4}{R}-S_1b_n^2\Big)e_1+S_1e_3,\\
K_{14}=A_2e_3-A_8b_n^2e_1,\quad K_{15}=(A_5+A_8)b_ne_1,\quad K_{21}=-(A_4+A_7)b_ne_2,\\
K_{22}=A_7e_2-\Big(A_1b_n^2+\dfrac{A_{10}}{R^2}\Big)e_0,\quad K_{23}=\Big(S_1b_n^2-\dfrac{A_1+A_{10}-\tau^{s+}-\tau^{s+}}{R}\Big)b_ne_0-S_1b_ne_2,\\
K_{24}=-(A_5+A_8)b_ne_2,\quad K_{25}=A_8e_2+\Big(\dfrac{A_{10}}{R}-A_2b_n^2\Big)e_0,\quad K_{31}=-\dfrac{A_4e_2}{R},\\
K_{32}=-\dfrac{(A_1+A_{10})b_ne_0}{R},\quad K_{34}=\Big(A_{10}-\dfrac{A_5}{R}\Big)e_2,\quad K_{35}=\Big(A_{10}-\dfrac{A_2}{R}\Big)b_ne_0,\\
K_{33}=\Big(A_{10}+\tau^{s+}+\tau^{s-}-\dfrac{S_1}{R}\Big)e_2-\Big((A_{10}+\tau^{s+}+\tau^{s-})b_n^2+\dfrac{A_1-\tau^{s+}-\tau^{s-}}{R^2}-\dfrac{S_1b_n^2}{R}\Big)e_0,\\
K_{41}=A_2e_3-A_8b_n^2e_1,\quad K_{42}=(A_5+A_8)b_ne_1,\quad K_{43}=\Big(\dfrac{A_5}{R}-A_{10}-S_2b_n^2\Big)e_1+S_2e_3,\\
K_{44}=A_3e_3-(A_9b_n^2+A_{10})e_1,\quad K_{45}=(A_6+A_9)b_ne_1,\quad K_{51}=-(A_5+A_8)b_ne_2,\\
K_{52}=A_8e_2+\Big(\dfrac{A_{10}}{R}-A_2b_n^2\Big)e_0,\quad K_{53}=-S_2b_ne_2+\Big(S_2b_n^2+A_{10}+\dfrac{h(\tau^{s+}-\tau^{s-})}{2R}-\dfrac{A_2}{R}\Big)b_ne_0,\\
K_{54}=-(A_6+A_9)b_ne_2,\quad K_{55}=A_9e_2-(A_3b_n^2+A_{10})e_0,\quad M_{11}=I_0f_1,\quad M_{13}=S_3e_1,\\
M_{14}=I_1f_1,\quad M_{22}=I_0f_0,\quad M_{23}=-S_3b_ne_0,\quad M_{25}=I_1f_0,\\
M_{33}=I_0f_0-\dfrac{S_3e_0}{R},\quad M_{41}=I_1f_1,\quad M_{43}=S_4e_1,\quad M_{44}=I_2f_1,\quad M_{52}=I_1f_0,\\
M_{53}=-S_4b_ne_0,\quad M_{55}=I_2f_0,\quad b_n=\dfrac{n}{R},\\
M_{12}=M_{15}=M_{21}=M_{24}=M_{31}=M_{32}=M_{34}=M_{35}=M_{42}=M_{45}=M_{51}=M_{54}=0,
\end{cases} \tag{B1}$$

where

$$e_0=(1+l^2b_n^2)\int_0^L X_m^2\mathrm{d}x-l^2\int_0^L\frac{\mathrm{d}^2X_m}{\mathrm{d}x^2}X_m\mathrm{d}x, \tag{B2}$$

$$e_1=(1+l^2b_n^2)\int_0^L\Big(\frac{\mathrm{d}X_m}{\mathrm{d}x}\Big)^2\mathrm{d}x-l^2\int_0^L\frac{\mathrm{d}^3X_m}{\mathrm{d}x^3}\frac{\mathrm{d}X_m}{\mathrm{d}x}\mathrm{d}x, \tag{B3}$$

$$e_2 = (1 + l^2 b_n^2) \int_0^L \frac{\mathrm{d}^2 X_m}{\mathrm{d}x^2} X_m \mathrm{d}x - l^2 \int_0^L \frac{\mathrm{d}^4 X_m}{\mathrm{d}x^4} X_m \mathrm{d}x, \tag{B4}$$

$$e_3 = (1 + l^2 b_n^2) \int_0^L \frac{\mathrm{d}^3 X_m}{\mathrm{d}x^3} \frac{\mathrm{d}X_m}{\mathrm{d}x} \mathrm{d}x - l^2 \int_0^L \frac{\mathrm{d}^5 X_m}{\mathrm{d}x^5} \frac{\mathrm{d}X_m}{\mathrm{d}x} \mathrm{d}x, \tag{B5}$$

$$f_0 = (1 + (ea)^2 b_n^2) \int_0^L X_m^2 \mathrm{d}x - (ea)^2 \int_0^L \frac{\mathrm{d}^2 X_m}{\mathrm{d}x^2} X_m \mathrm{d}x, \tag{B6}$$

$$f_1 = \left(1 + (ea)^2 b_n^2\right) \int_0^L \left(\frac{\mathrm{d}X_m}{\mathrm{d}x}\right)^2 \mathrm{d}x - (ea)^2 \int_0^L \frac{\mathrm{d}^3 X_m}{\mathrm{d}x^3} \frac{\mathrm{d}X_m}{\mathrm{d}x} \mathrm{d}x. \tag{B7}$$